Gravity on the Bruhat-Tits Tree

Daniel S. Gift

May 1, 2017

Advised by Professor Steven S. Gubser
Department of Physics
Princeton University

A senior thesis submitted to the Princeton University Department of Physics in partial fulfillment of the requirement of a Bachelor of Arts degree.

This paper represents my own work in accordance with University regulations.

Daniel Steven Gift

Gravity on the Bruhat-Tits Tree

Daniel S. Gift
Advised by Professor Steven Gubser

Abstract

It has been noted that the set of p-adic numbers and the Bruhat-Tits tree serve as a useful pairing of boundary and bulk on which a theory of AdS/CFT can be formulated. In this thesis, we assume there are two fields that live on the tree: a scalar matter field and a graviton field. We compute bulk-to-boundary propagators for both fields as a first step towards calculating how their behavior in the bulk corresponds with the CFT side of the duality. We also extend a formulation of the theory of gravity on this tree developed by Gubser et al. [1] to include these scalars, and we explore perturbative solutions to the resulting Einstein equation on the tree. We find that our solutions depend on the geometry of our fields, but for fields with reasonable symmetry, we find solutions that are consistent with expectations about how the fields should act at the boundary. This is true even when we introduce the notion of a Euclidean black hole on the tree, which is represented as a loop in the tree. Though these solutions are arrived at via pertubative methods, in some circumstances they are valid and bounded throughout the entirety of the tree. Furthermore, we find these solutions correspond to adding relevant operators to our conformal field theory, and because the renormalization group flow in our CFT has a low-energy cutoff in some of our geometries, set by the existence of a "center" of our tree, this shows that we will not flow out of the perturbative regime and can take our perturbative solutions as reliable throughout the tree.

Acknowledgements

This thesis is more than a book; it represents the culmination of a 4-year-long journey through the insanity that is a physics education. It has been a whirlwind and a blast, and it is only appropriate to thank the people who have made it so successful.

I am incredibly indebted to my advisor, Professor Gubser, for taking me on, working with me through the year and patiently helping me to get up to speed on research topics above my current physics education level. His clear way of explaining things when I didn't know something (even when perhaps I should have) made the learning process much easier. His careful and thoughtful comments on my work throughout the year, and especially on my thesis draft, have been invaluable.

I also want to thank the graduate students who have helped me to understand what was going on in the research group. I in particular want to thank Sarthak Parikh for taking his time on numerous occasions to meet with me and clarify concepts I found confusing.

I would be remiss if I did not also thank the physics professors who have shaped my education and research experiences here at Princeton. Thank you especially to Professors Verlinde and Klebanov for introducing me to and giving me a firm foundation in quantum field theory. I would also like to especially thank Professors Ji, Lisanti, and Marlow for their mentorship through summer research in my time as an undergraduate, teaching me how to think and work independently. I should also thank Professors Lisanti and Pretorius for their guidance as Junior Paper advisors, teaching me how to write a good scientific paper, how to do proper research and literature review, and how to present results in a professional way.

I would also like to thank my fellow physics peers for struggling through many many many long hours of problems sets. Thank you especially to Colin, Ethan, and J for being such supportive classmates time and time again and for helping me through more problem sets than I can count.

Thank you also to my roommates, Colin, Shubham, and Ethan, for putting up with me during thesis season. Thank you to Marisa, Eli, and Cecilia for your emotional support through the process, both directly and indirectly relating to thesis. A further thank you to Alice, for always being willing and ready to help me talk through things and for reading though my draft. A big thank you to N as well for not only reading through my entire thesis draft, but also for being a wizard at drawing and helping me make my figures.

Thank you to my parents and family for supporting me through all that I have done. You have shaped so much of who I am and who I aspire to be. Most importantly, thanks be to God for the gifts He has blessed me with me and for carrying me this far on my physics journey.

Contents

Chapter 1

Background and Motivation

One of the central goals of modern physics is to unify the four forces of nature. In particular, although quantum field theory (QFT) has described three of the forces with incredible accuracy and general relativity (GR) has described the fourth, QFT and GR are not compatible with each other. String theory, which posits that what we call particles are actually excitations of fundamental strings, has been proposed as a possible solution to this problem. The strings can either be closed strings, in which case they form loops, or they can be open strings. Physicists have discovered that certain vibrational modes of a closed string can be identified as a realization of a massless spin-2 particle. They concluded this particle must be the graviton, the which mediates the gravitational force. Furthermore, by applying conformal invariance constraints to string theory, physicists have produced the equations of motion for general relativity. More generally, closed strings exist in curved spacetimes that can approximately satisfy Einstein's relativity equations, suggesting that such strings are related to gravitons. Open strings, on the other hand, must have their ends attached to the higher-dimensional equivalents of strings, called D-branes, which can either take up a portion of or all of spacetime. The low energy dynamics of these open strings can be described by a Yang-Mills gauge theory, and consequently string theory has the potential to describe both gravity (via closed strings) and the other three forces (via open strings), which are wrapped up in Yang-Mills-like theories [2].

These developments were the backdrop to a major discovery, first written about by Maldacena in 1997 and expanded upon later by Gubser, Klebanov, and Polyakov, as well as by Witten, in 1998 [3] [4] [5]. These three papers form the backbone of the theory known as the AdS/CFT correspondance. This is a statement of equivalence between two theories that at first seem unrelated. On the AdS side, we have a theory of Anti de-Sitter spacetime that

follows the dynamical laws given by general relativity; note that an Anti de-Sitter space is a space with constant negative overall curvature (a consequence of the cosmological constant in Einstein's general relativity equations) [6]. On the CFT side, we have a conformal field theory, which is a field theory that is invariant under conformal transformations. For our purposes a conformal transformation is a translation in spacetime or an overall rescaling, but a somewhat more complete definition is a transformation that preserves angles but does not necessarily preserve lengths; for a much more complete treatment, see [7]. The early pioneers of AdS/CFT argued that these two theories were completely equivalent, and furthermore if the AdS space is in $n+1$ dimensions, the corresponding CFT is in n dimensions. As such, the CFT is generally associated with the boundary of the space on which the gravity theory is formulated, and the AdS space is often referred to as the "bulk." The power of this theory is that it has the potential to transform problems that may be difficult or intractable in one of these theories into an equivalent, possibly more tractable problem in the other theory.

Though the most commonly studied AdS/CFT correspondance is in $n = 4$ dimensions, it is applicable to any number of dimensions, and in particular this thesis is primarily concerned with the $n = 1$ case, in which our CFT has only one dimension and the corresponding AdS space has two. However, for our purposes here we would like to work with a discretized version of AdS space. Axenides, Floratos, and Nicolis discuss one way we might discretize AdS space, simply taking the discrete version of the group $SL(2,\mathbb{R})/U(1)$ that describes AdS space [8]. Note that $SL(2,\mathbb{R})$ is the special linear group, namely the group of 2×2 matrices with determinant 1 whose elements are in $\mathbb{R}$, and $U(1)$ is the group of 1×1 unitary matrices. However, Gubser et al. take this a step further and propose an alternative group representation of this discretization, using groups that involve p-adic numbers instead of ordinary real numbers; though the details are beyond the scope of this introduction, the reader is encouraged to read their Section 2.1 on this subject [9]. They point out, as others before them have [10] [11], that a natural realization of this discrete p-adic version of AdS space is the Bruhat-Tits tree, also known as the Bethe lattice. The definition of what the p-adic numbers are, and what their relationship to the Bruhat-Tits tree is, will be explained in the next chapter, but for now suffice it to say that the p-adic numbers are a set of numbers analogous to the real numbers defined in relation to some prime number p, and the Bruhat-Tits tree is a lattice with a tree-like structure whose boundary can be identified with the p-adic numbers.

In this thesis, we will explore primarily the bulk side of this p-adic AdS/CFT theory,

with some references to the CFT throughout, especially in Section 6.4. In Chapter 2, we provide an intoduction to p-adic numbers and their relationship to the Bruhat-Tits tree. In Chapter 3, we introduce a scalar field ϕ on the lattice and we compute its propagators, both in the bulk and from the bulk to the boundary. In Chapter 4, we introduce the concept of the graviton on the tree, which corresponds to non-constant edge lengths, and we calculate its propagators as well. In Chapter 5, we introduce and derive more generally the concept of general relativity and Einstein's equation as applied to the Bruhat-Tits tree. In Chapter 6, we introduce three possible kinds of solutions to the equations of motion established in Chapter 5; all three are arrived at perturbatively. In Chapter 7, we present our conclusions and suggest avenues for further research.

The main results from this thesis are the inclusion of a matter field in the Einstein equation of motion on the tree (Eqn. 5.14) and three perturbative solutions to the set of equations of motion, which consists of the Einstein equation and the Klein-Gordon equation for the scalar field (Eqn. 5.15). A particularly interesting result is that some of these perturbative solutions, namely those in which we assume some form of radial symmetry, remain bounded throughout the entirety of the tree. This work also demonstrates that for a negative quadratic scalar term in the action, a term which we find is required by our well-controlled radial solutions, the corresponding operator on the CFT side of the correspondance is relevant. Furthermore, the associated renormalization group flow is cut off when we assume a radially symmetric geometry, suggesting that in these cases, the fields will not flow out of the perturbative regime.

Chapter 2

Mathematical Background

Before we begin our calculations with p-adic numbers on the Bruhat-Tits tree, we first take some time to familiarize ourselves with what the p-adics and the Bruhat-Tits tree are. This chapter is far from a complete coverage of these topics; rather this introduces only the minimal amount of information necessary to understand the calculations done in the rest of this thesis. For a more complete overview, see [12].

2.1 p-adic Numbers

In general, a p-adic number can often be thought of as an expression of an ordinary real number; however, the p-adic norm is different from the ordinary norm. Specifically, p-adics are expressed in terms of some prime number p. As such, we can have 2-adic, 3-adic, or 7-adic numbers; we write p-adic for the general case of any prime p. p-adics are written as if they are a number in base p: the number is represented as a string of digits (possibly with a decimal point) where each digit is an integer between 0 and $p-1$, inclusive. We represent this formally as

$$x = \sum_{n=v(x)}^{\infty} a_n p^n = p^{v(x)} \sum_{n=0}^{\infty} b_n p^n, \tag{2.1}$$

where the a_n are nonnegative integers less than p, $b_n = a_{n-v(x)}$, and x is a p-adic number. We start picking digits at some arbitrary finite place, which we represent for any given p-adic number x as the function $v(x)$; therefore all digits in the $p^{v(x)-1}$place and further right are 0.

We now introduce the p-adic norm, which is

$$|x|_p \equiv p^{-v(x)}. \tag{2.2}$$

This means that some numbers conventionally thought of as larger have a smaller p-adic norm. For example, in the 3-adics, we would write 36 as

$$36 = 3^2 \left(1 \cdot 3^1 + 1 \cdot 3^0\right),$$

where we see here that $p = 3$, $v(x) = 2$, $b_0 = 1$, $b_1 = 1$, and $b_n = 0$ for all $n \geq 2$, so the p-adic norm $|36|_3 = 3^{-2} = \frac{1}{9}$. Compare this to the 3-adic norm for 3, which is simply 1, and we see that 36 actually has a smaller 3-adic norm than 3. In particular, the more powers of p that a number is divisible by, the smaller its p-adic norm. Note that this means the p-adic norm of a number is not unique; for example, all numbers prime relative to p will have the same norm, p^0, because all these numbers must have a non-zero digit in the p^0 place. Similarly, all number divisible by p but not by p^2 will also have the same norm as each other, namely p^{-1}.

The p-adics are a closed set, insofar as there is a unique multiplicative and additive inverse to every element in the set, as well as a multiplicative identity, 1, and an additive identity, 0 (Note that we define $|0|_p = 0$). We denote this entire subset of p-adic rationals as $\mathbb{Q}_p$. We also naturally define the p-adic integers as numbers with no digits in places smaller than p^0, which means these are numbers with $v(x) \geq 0$, or equivalently, $|x|_p \leq 1$; we denote this set of p-adic integers as $\mathbb{Z}_p$. Furthermore, we define the p-adic units, $\mathbb{U}_p$, as the subset of the integers with $|x|_p = 1$. We can therefore express the non-zero p-adics, $\mathbb{Q}_p^\times$, as

$$\mathbb{Q}_p^\times = \bigcup_{n \in \mathbb{Z}} p^n \mathbb{U}_p. \tag{2.3}$$

This is best conceptualized with the idea that $\mathbb{Q}_p$ is a space of numbers arranged around the origin based on p-adic norm, with numbers that have a larger norm being further away. Then $\mathbb{Z}_p$ is the unit ball, and $\mathbb{U}_p$ is the unit sphere, and Eqn. 2.3 is a statement that we can cover the entire space except the origin with an infinite set of nested, scaled spheres.

2.2 The Bruhat-Tits Tree

We can relate the p-adic numbers to a tree, known in the math community as the Bruhat-Tits tree or in the physics community as a Bethe lattice. This tree has coordination number $p+1$, which means each vertex on the tree has $p+1$ points that it is directly connected to. For now it is most convenient to think of the tree as having a definite "upward" direction, in which each node is connected to one node below it and p connected nodes above it. This

means that there p times as many nodes in a level than in the level immediately below it; see Fig. 2.1 for a visual guide. We then associate the p-adic numbers with the tree by having each level of the tree specify a different digit of a p-adic number. Since each node has p upward branches, each branch corresponds to choosing one of the p possible digits that could be chosen for the digit in that place in the number, as shown in Fig. 2.1 using the 3-adics. Typically we choose a convention such that the left-most branch is the 0 digit, and the digits increase as we move right in the branches.

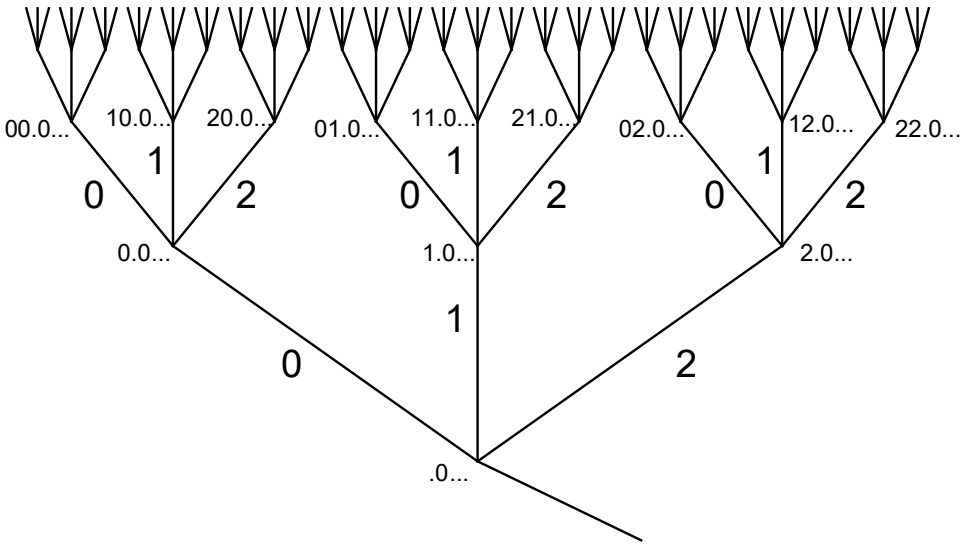

Figure 2.1: *A 3-adic Bruhat-Tits tree, in which we see each upward branch corresponds to choosing a digit: 0, 1, or 2. We also see the coordination number is 4: each node has 3 upward connections and 1 downward connection. The numbers next to each vertex indicate the incomplete p-adic number we have so far built up, having specified all the digits to the right of those shown. The "..." indicates that the non-written digits are all 0.*

To construct a full p-adic number on this tree, we postulate that we start picking our digits infinitely to the right of the decimal, and therefore infinitely far down in the tree, but as we move up the tree we pick 0 without fail until a certain specified place (specifically, until we reach the $p^{v(x)}$ place). If we consider the Bruhat-Tits tree to extend infinitely in both upward and downward directions, this corresponds to starting infinitely far down and traversing upward using only the leftmost branch at each node until we reach some point that we will associate with $p^{v(x)}$. From here on we are free to pick any combination of digits as we continue to move up the tree. In practice we will often only pick a few non-zero digits before returning to always picking zeros for our digit so that our p-adic number is convenient to write.

As we take a step up in the tree, traversing up through the "levels," we imagine that each step specifies a digit of a p-adic number. We can thus associate each level with a power of p: at any given level, which we will label as the p^ω level (where ω is an integer), we can say we have specified the p-adic number up to the $p^{\omega-1}$ place, or in other words, the p^ω place is the right-most unspecified place. Because the p-adic concept of size, or norm, is the inverse of the traditional notion, we see that leaving further-left digits unspecified corresponds to leaving smaller corrections to our estimate of the number unspecified, in the same way that specifying π as 3.14 without specifying any digits further right leaves smaller corrections to our estimate of π unspecified.

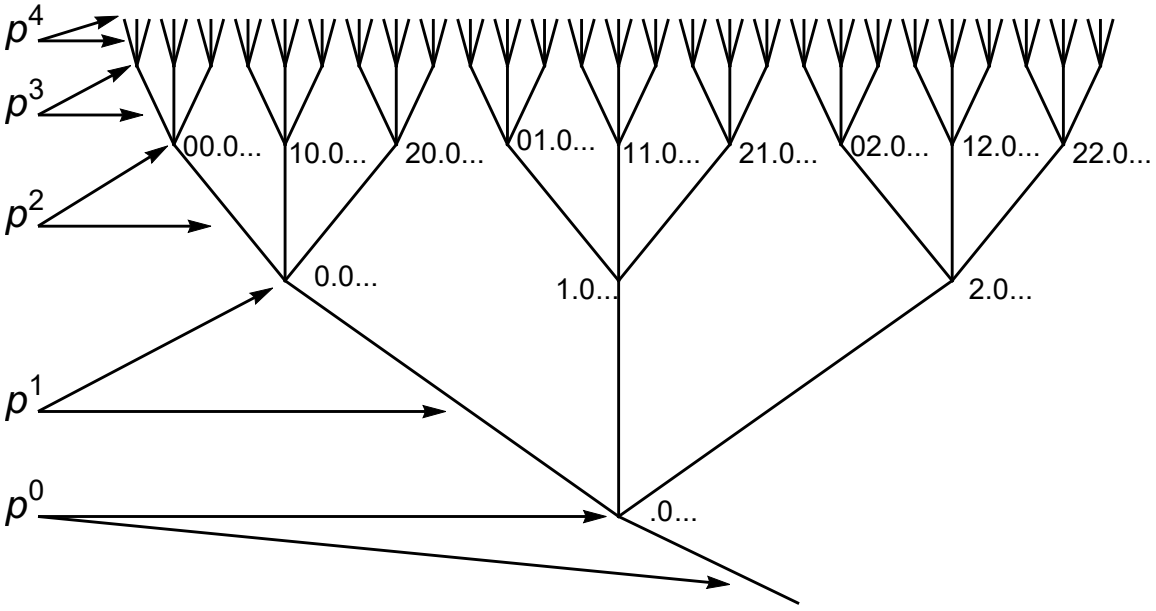

Figure 2.2: *A 3-adic Bruhat-Tits tree showing that we can label the depth of our vertices and our edges by powers of p. Note that at level p^ω, a p-adic number is specified up to, but not including, the p^ω place. These p^ω values along the left side of the figure are the z_0 values of these particular vertices and edges.*

From this perspective, we note that infinitely far up the tree, we can specify p-adic numbers with infinite precision, and therefore we can consider the set of p-adic numbers to be given by the upper boundary of the Bruhat-Tits tree. Indeed, we see clearly that taking the left branch at every intersection will eventually give us the p-adic number 0, with 0 as all its digits. We also add to this the notion that the bottom of the tree infinitely far down is the p-adic ∞. There is one unique path on the tree from ∞ to every p-adic number on the upper boundary of the tree, and as we traverse this path we will specify that number

with ever-increasing accuracy by picking digits further and further to the left. Much of this is represented in Fig. 2.2, including the concept of partially-specified p-adic numbers and the concept of the depth labeling.

If we consider a p-adic number at the boundary of the tree and we ask about its p-adic norm, we see that its norm is given by the rightmost non-zero digit, which in other words is the first time in the path that we choose a branch that is not the 0 branch. Let us call the leftmost edge of the tree, the path that goes from ∞ to 0, the trunk of the tree. Then we can specify the norm of a p-adic number by where the path to that number diverges from the trunk. In fact, all numbers with the same norm diverge from the trunk at the same node. We consider the entire segment of the tree that diverges from the trunk at a given point to be a "bush", and we say that this bush is "rooted" at p^ω, where p^ω is the depth of point at which the bush connects to the trunk, and $p^{-\omega}$ is the norm of every p-adic number in that bush. Fig. 2.3 gives a visualization of this.

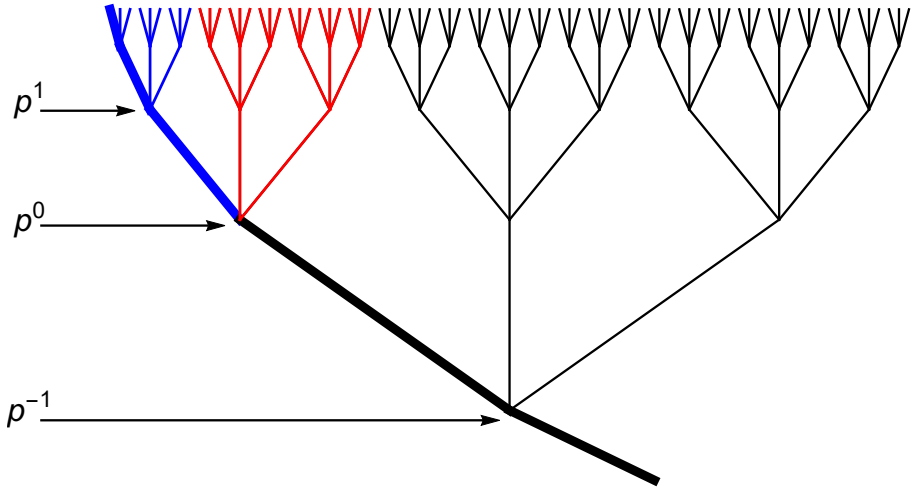

Figure 2.3: *A schematic representation of the trunk and a bush on the tree. The trunk is the thick part of the tree, and the part of the tree in red is one bush. The bush shown here in particular is the set of all units $\mathbb{U}_p$, as it contains all numbers of norm $p^{-0} = 1$. The union of the red and blue parts of the tree represents the set of all p-adic integers, $\mathbb{Z}_p$, as they contain all numbers with norm ≤ 1.*

We return to the concept introduced earlier that the p-adic numbers can be broken up into an infinite set of scaled copies of $\mathbb{U}_p$. We see that the association of the p-adics with the tree gives another way of visualizing this breakdown, because the p-adic numbers at the top of every bush correspond to a copy of $\mathbb{U}_p$ multiplied by the depth of the bush's root. That is, at every node on the trunk, the bush emerging from that node looks like a

copy of the one that contains $\mathbb{U}_p$, and these copies are distinguished only in where they are rooted. The higher a bush is rooted, the larger our $v(x)$ and the more zeros we have chosen for further-right digits, meaning the more p's we multiply by before we find any non-zero digits. Since $\mathbb{U}_p$ corresponds to non-zero digits in the p^0's place, this means each higher bush contains $\mathbb{U}_p$ multiplied by higher and higher powers of p.

Finally, we will find it useful later in this thesis to introduce notation to specify a point z on the tree as an ordered pair (z_n, z_0), where z_0 is a depth coordinate (p^ω for some integer ω) and z_n is a full, infinitely-specified p-adic number at the edge of the tree that can be reached by moving only directly upwards in the tree from the point z. Another way of saying this is that the point $z = (z_n, z_0)$ specifies the number z_n up to accuracy z_0, where z_0 is the place of the first digit that is unspecified. While this does not provide a unique labeling for every point on the tree, this will be convenient to help us regardless. As an example, we note that any point on the trunk can be expressed as $(0, z_0)$, since we can reach 0 by continuing directly up the trunk. We will also find it useful to talk about the depth of certain edges as well as the depth of certain nodes; thus we associate each edge with the (z_n, z_0) values that are assigned to its upper node (as shown in Fig. 2.2). Since each node has only one lower edge (though many upper edges), this association seems most natural, as it gives us a one-to-one correspondance of edge and vertex labeling.

2.3 Integration

We will find it useful near the end of this thesis to perform p-adic integrals, and so we review the mechanism for doing so here. Our approach will be to break the domain of $\mathbb{Q}_p$ into pieces over which the integrand will be constant, and in doing so we will transform the integral into a sum which we can more easily compute.

Before we begin our discussion of p-adic integration, it will be helpful to define a set S_μ^ω such that

$$S_\mu^\omega = \left\{ x \in \mathbb{Q}_p \colon x = \sum_{n=\mu}^{\omega-1} a_n p^n,\ a_n \text{ is integer between 0 and } p-1 \right\} \tag{2.4}$$

when $\omega > \mu$ and $S = \{\emptyset\}$ for $\omega \leq \mu$. Then S is the set of all the points on the Bruhat-Tits tree that are $\omega - \mu$ steps up the tree from the trunk point at depth p^μ. We can best understand this by example, using Fig. 2.2 as a visual guide. Consider $\mu = 0$, $\omega = 2$ on the 3-adics. Then we consider all numbers made up of digits in the 2^0 and the 2^1 place,

which would be $\{00, 01, 02, 10, 11, 12, 20, 21, 22\}$. These are all points on the tree that can be accessed by starting at the p^0 level and moving up $\omega - \mu = 2 - 0 = 2$ steps. This is thus the set of all points at the ω level that connect with the trunk at or above the μ level.

We now consider an integral as a Riemann sum of the form

$$\int_{\mathbb{Q}_p} dx f(x) \approx \sum_{x \in S_\mu^\omega} p^{-\omega} f(x), \tag{2.5}$$

where we assume $f(x)$ goes to 0 sufficiently quickly when $|x|_p$ is large. True integration would happen by summing over all values of x at upper edge of the tree, where the p-adic numbers are located, but instead we restrict the nodes to be only at a certain finite height ω, which we will later take the limit as $\omega \to \infty$ so that we truly are integrating over the p-adics. We also restrict the nodes to only be those in bushes that are rooted at or above the μ level, with the idea that if $f(x)$ vanishes sufficiently quickly in the regime of $|x|_p \gg 1$, we can ignore contributions from anything in which $|x|_p > \mu$, which corresponds to numbers rooted lower than μ. Thus, we can cut off our sum without taking μ all the way to $-\infty$ and still retain effectively the same result. In the limit that $\mu \to -\infty$ and $\omega \to \infty$, Eqn. 2.5 becomes an exact equality.

Using this, we compute some general integrals. We note that

$$\int_{\mathbb{Z}_p} dx = \lim_{\omega \to \infty} \sum_{x \in S_0^\omega} p^{-\omega}, \tag{2.6}$$

since an integral over the p-adic integers is an integral over the p-adic rationals that are rooted at p^0 or higher in the Bruhat-Tits tree, a requirement satisfied by setting $\mu = 0$.We can also determine that there are $p^{\omega-\mu}$ nodes in S_μ^ω, since at each level we have p times as many nodes as in the level below it. This means our sum in Eqn. 2.6 becomes

$$\int_{\mathbb{Z}_p} dx = \lim_{\omega \to \infty} p^{\omega - 0} p^{-\omega} = 1. \tag{2.7}$$

We also note that

$$\int_{\alpha S} f(x) dx = |\alpha|_p \int_S f(\alpha y) dy \tag{2.8}$$

where α is some p-adic number and S is some set (like $\mathbb{Q}_p$ or $\mathbb{Z}_p$), such that αS means that α multiplies every element in the set S. We justify this by using the substitution $x = \alpha y$ and so noticing that a change of variables from x to y gives an extra factor of $|dx/dy|_p = |\alpha|_p$. Finally, we observe that we can obtain the p-adic units $\mathbb{U}_p$ by taking the set of integers and

removing from it all integers that are divisible by p; that is,

$$\mathbb{U}_p = \mathbb{Z}_p \backslash (p\mathbb{Z}_p). \tag{2.9}$$

We can then combine Eqns. 2.7, 2.8, and 2.9 to find

$$\int_{\mathbb{U}_p} dx = \int_{\mathbb{Z}_p} dx - \int_{p\mathbb{Z}_p} dx = 1 - |p| \cdot 1 = 1 - \frac{1}{p}. \tag{2.10}$$

These basic integrals will be all that is necessary for us to perform more general integrals later. In particular, the approach we will take is to turn our integrand into a sum of functions, each of which is constant over $\mathbb{U}_p$. This will allow us to take the summation and the entirety of the integrand outside of the integral and will leave us just with an integral of the form of Eqn. 2.10. Then we will be left merely with an infinite sum, which we will be able to compute using the rules of geometric series.

Chapter 3

Matter Fields on the Tree

Equipped with the mathematical understanding of the Bruhat-Tits tree and its relation to the p-adic numbers, we now turn to applying this machinery to physics, and specifically to calculating the behavior of a matter particle moving on the tree. Specifically, we take the tree as a kind of lattice in spacetime, such that the field corresponding to our matter particle can take on different values at different vertices on the tree. We denote the scalar matter field as ϕ and refer to its value at a specific vertex x as $\phi(x)$. We will often abbreviate this as ϕ_x.

We start with a Lagrangian for this particle, for which we choose the simplest massive Lagrangian:

$$\mathcal{L}_\phi = \frac{1}{4}\sum_{y\sim x}(\phi_x - \phi_y)^2 + \frac{1}{2}r\phi_x^2. \tag{3.1}$$

The second term is a mass term for the ϕ field, and we can associate the mass of the particle with the coefficient of this term, namely

$$m_\phi^2 \equiv r \tag{3.2}$$

The first term in our Lagrangian is the kinetic term, where we consider the expression $(\phi_x - \phi_y)$ to be similar to a derivative on our discrete tree. Points x and y are neighbors, which is to say, they are connected to each other on the tree by a single edge. Just taking $(\phi_x - \phi_y)$ picks out a specific neighbor of x, however, and so to be democratic we must sum over all neighbors of x, thus giving us the first term in Eqn. 3.1. The notation $y \sim x$ indicates we are summing over all y's that are neighbors of x.

We can now obtain an action from the Lagrangian given by Eqn. 3.1; we do this by summing the Lagrangian over all points on the tree x, in analogue to integrating over all of

spacetime as is done in regular QFT. Thus we get

$$S_\phi = \sum_x \left(\frac{1}{4} \sum_{y \sim x} (\phi_x - \phi_y)^2 + \frac{1}{2} m_\phi^2 \phi_x^2 \right). \tag{3.3}$$

We can write this in a somewhat more intuitive form by noting that summing over all neighbors of every point on the tree is equivalent to summing over the endpoints of every edge of the tree, except that the former double-counts every pairing (for every pair, we have a term when the first point is x and the second is y, and a term when the second point is x and the first is y). Thus, we can rewrite Eqn. 3.3 as

$$S_\phi = \frac{1}{2} \sum_{\langle xy \rangle} (\phi_x - \phi_y)^2 + \frac{1}{2} \sum_x m_\phi^2 \phi_x^2. \tag{3.4}$$

The notation $\langle xy \rangle$ indicates a summation over every pair of vertices x and y such that the two vertices are neighbors; equivalently, $\langle xy \rangle$ specifies an edge whose endpoints are x and y.

We now would like to obtain an equation of motion for ϕ, which we get by picking a specific vertex ϕ_z and varying the actions with respect to it. Starting with Eqn. 3.4, we can say that, since our choice as to which vertex to call x and which to call y is arbitrary, we can label the vertex z as x every time z is one of the vertices involved in a term of the sum. Thus, we are left with varying ϕ_z in the expression

$$\frac{1}{2} \sum_{y \sim z} (\phi_z - \phi_y)^2 + \frac{1}{2} m_\phi^2 \phi_z^2 \tag{3.5}$$

which leads us to the equation of motion

$$\sum_{y \sim x} (\phi_x - \phi_y) + m_\phi^2 \phi_x = 0, \tag{3.6}$$

where we have relabeled z as x. A visual representation of this is presented in Fig. 3.1.

This motivates us to introduce a shorthand for the Laplacian on the tree:

$$\Box \phi_x \equiv \sum_{y \sim x} (\phi_x - \phi_y), \tag{3.7}$$

meaning our equation of motion becomes simply

$$\Box \phi_x + m_\phi^2 \phi_x = 0. \tag{3.8}$$

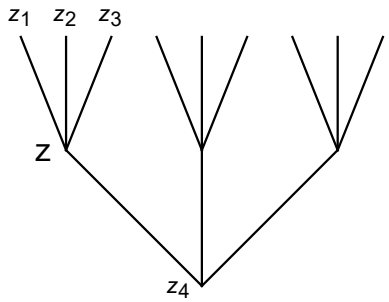

Figure 3.1: *If we pick a vertex such as the one labeled here by z, then summing over all neighbors requires adding contributions from z_1, z_2, z_3, and z_4. Since the sum in Eqn. 3.4 is represented as a sum over edges $\langle xy \rangle$, in each case we consider z to be the x vertex and z_i to be the y vertex.*

We now move on to calculating the propagator for this field. Though this is an interesting result in and of itself, we are additionally motivated by the fact that in AdS/CFT, particles in the CFT, at the boundary of the Bruhat-Tits tree, travel to other points on the boundary by descending into the tree and then ascending back up to a different point on the boundary. Consequently, the propagator of ϕ from the boundary to the bulk is an important tool in determining the propagator and higher-order correlation functions in the conformal field theory as well. Athough we will not perform any of these correlation function calculations in this thesis, having these expressions is useful for others to later perform these calculations. Gubser et al. [9] have already calculated these propagators for the ϕ field, but we go through the work here explicitly as a model for the graviton field in the next chapter.

3.1 Bulk-to-Bulk ϕ Propagator

We would like to work out a propagator for ϕ in the bulk of the tree (namely, the propagator between two points somewhere in the middle of the tree, not on the boundary), as both a useful tool for the field theory and in preparation for the bulk-to-boundary propagator in the next section.

Propagators are also Green's functions of the equations of motion, and so to find our propagator, we look for a Green's function that satisfies the equation

$$\left(\Box + m_\phi^2\right) G_\phi(x, y) = \delta(x, y). \tag{3.9}$$

$\delta(x, y)$ is the Kronecker delta function for vertices, equal to 1 if x and y are the same vertex

and equal to 0 if they are not. $G(x, y)$ is a function such that

$$\sum_y G_\phi(x, y) J_s(y) = \phi(x) \tag{3.10}$$

for some source field J_s, in analogue to the continuous case for Green's functions. To solve this, we note that for $x \neq y$,

$$\sum_{z \sim x} G_\phi(x, y) - G_\phi(z, y) = -m_\phi^2 G_\phi(x, y), \tag{3.11}$$

and for $x = y$ we have

$$\sum_{z \sim y} G_\phi(y, y) - G_\phi(z, y) = -m_\phi^2 G_\phi(y, y) + 1. \tag{3.12}$$

We take as an ansatz that

$$G_\phi(x, y) = A p^{-\Delta_\phi d_\phi(x,y)}, \tag{3.13}$$

where $d_\phi(x, y)$ is the distance function between two vertices and counts the number of edges separating x and y, Δ_ϕ is a constant related to the mass and which we will see in Section 6.4 is also related to the scaling dimension of an operator in the corresponding CFT, and A is some scaling constant. Plugging this ansatz into Eqn. 3.11, we see

$$\begin{aligned} A\left((p+1)\, p^{-\Delta_\phi d_\phi(x,y)} - (p)\, p^{-\Delta_\phi [d_\phi(x,y)+1]} - p^{-\Delta_\phi [d_\phi(x,y)-1]}\right) &= -A m_\phi^2 p^{-\Delta_\phi d_\phi(x,y)} \\ \Rightarrow \left((p+1) - p^{1-\Delta_\phi} - p^{\Delta_\phi}\right) &= -m_\phi^2. \end{aligned} \tag{3.14}$$

To get this, we note that for a given y, there is a path from x to y, and one of the neighbors of x will be on this path. Thus, there will be one neighbor of x that will be one step closer to y than x is; this is the third term on the left hand side. The other p neighbors will be a step in the wrong direction and so will be one step further away from y than x is, as represented by the second term. From Eqn. 3.14, we can solve for m_ϕ^2:

$$m_\phi^2 = -\left(1 - p^{\Delta_\phi}\right)\left(1 - p^{1-\Delta_\phi}\right) = -\frac{1}{\zeta_p(-\Delta_\phi)\zeta_p(\Delta_\phi - 1)} \tag{3.15}$$

where in the last equality we define the p-adic ζ function as

$$\zeta_p(x) \equiv \frac{1}{1 - p^{-x}}. \tag{3.16}$$

We can also plug our ansatz into Eqn. 3.12 to obtain the equation

$$A\left((p+1)-(p+1)\,p^{-\Delta_\phi}\right) = -Am_\phi^2 + 1, \tag{3.17}$$

which we obtained by noting that every neighbor of y is one step away from y regardless of direction. From Eqn. 3.17 and plugging in our result from Eqn. 3.15, we can now solve for A:

$$A = \frac{1}{(p+1)\left(1-p^{-\Delta_\phi}\right)-\left(1-p^{\Delta_\phi}\right)\left(1-p^{1-\Delta_\phi}\right)} = \frac{1}{p^{\Delta_\phi}\left(1-p^{-2\Delta_\phi}\right)} = \frac{\zeta_p(2\Delta_\phi)}{p^{\Delta_\phi}}. \tag{3.18}$$

Thus, we ultimately find

$$G_\phi(x,y) = \frac{\zeta_p(2\Delta_\phi)}{p^{\Delta_\phi}} p^{-\Delta_\phi d_\phi(x,y)}. \tag{3.19}$$

This is the propagator for ϕ in the bulk of the lattice.

3.2 Bulk-to-Boundary ϕ Propagator

$G_\phi(x,y)$ tells us the propagator from one point x on the tree to another point y on the tree, but now we would like to extend this and find the propagator $K_\phi(x,a)$ for a particle that goes to a point a on the boundary of the tree. This can most easily be done by sending our point y to the boundary in Eqn. 3.19; namely

$$K_\phi(x_n, x_0; a_n) = \lim_{|a_0|_p \to 0} |a_0|_p^{-\Delta_\phi} G_\phi(x, a^*), \tag{3.20}$$

where the factor of $|a_0|^{-\Delta_\phi}$ is inserted for convergence, as we will see later. Here, we have adopted the convention that vertices labeled by letters from the beginning of the alphabet represent boundary vertices, and those from the end of the alphabet represent bulk vertices, while the point a^* represents a point in the bulk with the same a_n as the boundary point a, but with a non-zero depth a_0. In the limit where $|a_0|_p \to 0$, a^* approaches a. Furthermore, here we switch to using the labeling method introduced at the end of Section 2.2, where a vertex x can be represented by an ordered pair of its depth x_0 and a p-adic number x_n that can be reached by going directly up to the top of the tree from x. Our omission of a reference to a_0 in the argument of K_ϕ is meant to indicate that the vertex we are interested is in fact on the boundary, and so can be represented just by the p-adic number on the boundary to which it corresponds. Note the distinction we make here: x_n is the p-adic number that we have associated with a bulk vertex, x_0 is the depth of the vertex in question, and x is a

label for the vertex itself.

We now would like to explicitly compute the limit

$$K_\phi(x_n, x_0; a_n) = \frac{\zeta_p(2\Delta_\phi)}{p^{\Delta_\phi}} \lim_{|a_0|_p \to 0} |a_0|_p^{-\Delta_\phi} p^{-\Delta_\phi d_\phi(x_n, x_0; a_n, a_0)}. \tag{3.21}$$

We cannot proceed, however, without a more explicit definition of $d_\phi(x_n, x_0; a_n, a_0)$.

3.2.1 Distance Between Vertices

First, we assume that there is no direct path in the tree from x to the point at ∞ that passes through a^*; if there is, we switch the x and a^* labels such that it is no longer true. Now, there are two scenarios: either the path from a^* to ∞ passes through x, or it does not. The first situation is shown in Fig. 3.2, while the second is shown in Fig. 3.3.

In the first case, the calculation is easy, since to get from a^* to x we must simply go down a certain number of steps. Thus, the distance between the points is given by the difference in depths, or, expressed exponentially,

$$p^{-d_1(x,a^*)} = \frac{|a_0|_p}{|x_0|_p} \tag{3.22}$$

where the subscript 1 indicates this is the distance measure in the first case. A graphical example of this setup is given in Fig. 3.2.

In the second case, to get from x to a^*, we must first traverse down the tree to some common anscestor of x and a^*, then back up. Let us call this common anscestor m; m will be the highest vertex that both points include in their path to ∞. The depth of m will also specify the right-most digit at which a_n and x_n will differ, because for further-right digits, the path on the tree for both will be identical (and thus their digits will be identical). Thus, the depth of m will be $|a_n - x_n|_p^{-1}$. Therefore, our total distance traveled will be the distance we need to travel from x to m plus the distance we need to travel from a^* to m, i.e.

$$p^{-d_2(x,a^*)} = \left(\frac{|a_0|_p}{|a_n - x_n|_p}\right)\left(\frac{|x_0|_p}{|a_n - x_n|_p}\right) = \frac{|a_0|_p |x_0|_p}{|a_n - x_n|_p^2}. \tag{3.23}$$

We can see how this works visually in Fig. 3.3.

Mathematically, we can distinguish between the two above scenarios by comparing $|x_0|_p$ and $|a_n - x_n|_p$. Since we must "descend" the tree from x to reach the common ancestor in the second case, we know the second case is true iff $|x_0|_p < |a_n - x_n|_p$ (that is, if the level specified by $|a_n - x_n|_p$ is lower in the tree than x) . If, on the other hand, $|x_0|_p \geq |a_n - x_n|_p$,

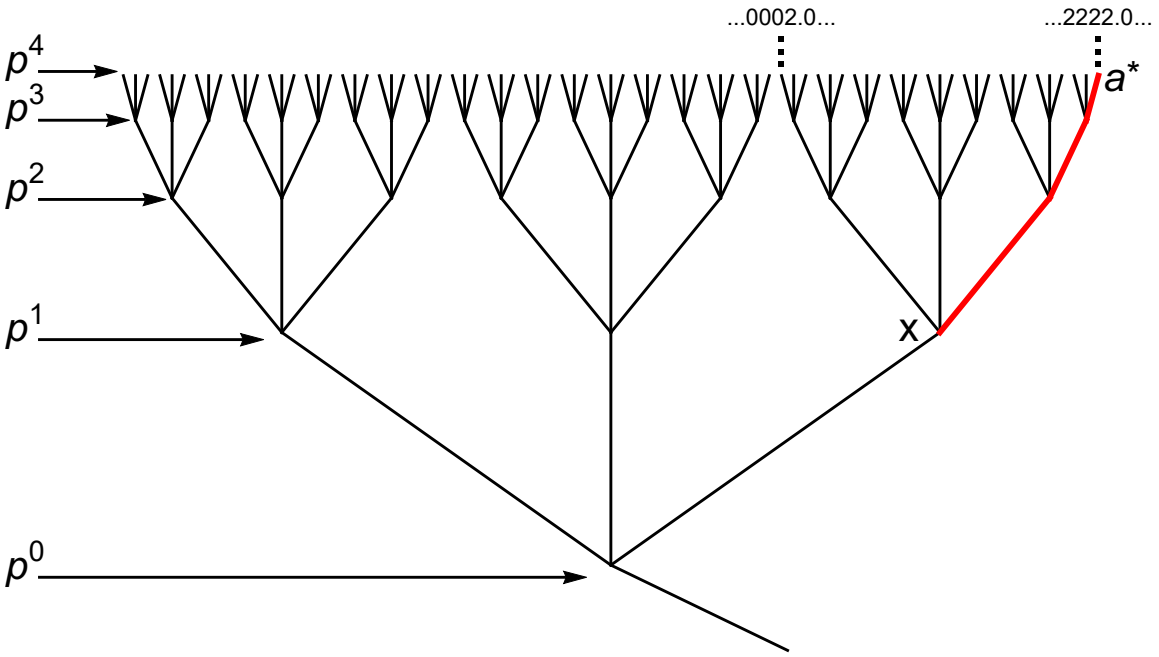

Figure 3.2: *A visual example of the first case, in which x is on the path from a^* to ∞, which we see here clearly because in order to travel from a^* to the bottom outgoing branch, we must pass through x. We can also confirm Eqn. 3.22 in this example by noting that the distance, by counting the number of edges between a^* and x, is 3. This matches Eqn. 3.22:* $\frac{|a_0|_p}{|x_0|_p} = \frac{p^{-4}}{p^{-1}} = p^{-3} = p^{-d_1(x,a^*)}$.

this means that x_n and a_n share digits up to the x_0 place (or more), meaning that x is on the path from a^* to the point at ∞. We can confirm this with the examples in Figs. 3.2 and 3.3. For Fig. 3.2, which shows the first case, we see that $|x_0|_p = p^{-1}$ and $|a_n - x_n|_p = |2222.0 - 0002.0|_p = p^{-1}$, so $|x_0|_p \geq |a_n - x_n|_p$. On the other hand, for Fig. 3.3, which represents the second case, $|x_0|_p = p^{-3}$ and $|a_n - x_n|_p = |2222.0 - 0020.0|_p = p^{-1}$, so $|x_0|_p < |a_n - x_n|_p$. Thus, we find that

$$p^{-d_\phi(x,a^*)} = |a_0|_p |x_0|_p \begin{cases} \frac{1}{|a_n - x_n|_p^2}, & |a_n - x_n|_p > |x_0|_p \\ \frac{1}{|x_0|_p^2} & |x_0|_p \geq |a_n - x_n|_p \end{cases}, \tag{3.24}$$

which we can rewrite as

$$p^{-d_\phi(x,a^*)} = \frac{|a_0|_p |x_0|_p}{\sup|(x_0, a_n - x_n)|_p^2}, \tag{3.25}$$

where the supremum norm $\sup|(\alpha, \beta)|_p$ is equal to $|\alpha|_p$ if $|\alpha|_p \geq |\beta|_p$ and $|\beta|_p$ if $|\beta|_p > |\alpha|_p$.

Finally, we are equipped to return to and simplify Eqn. 3.21. We see that we must

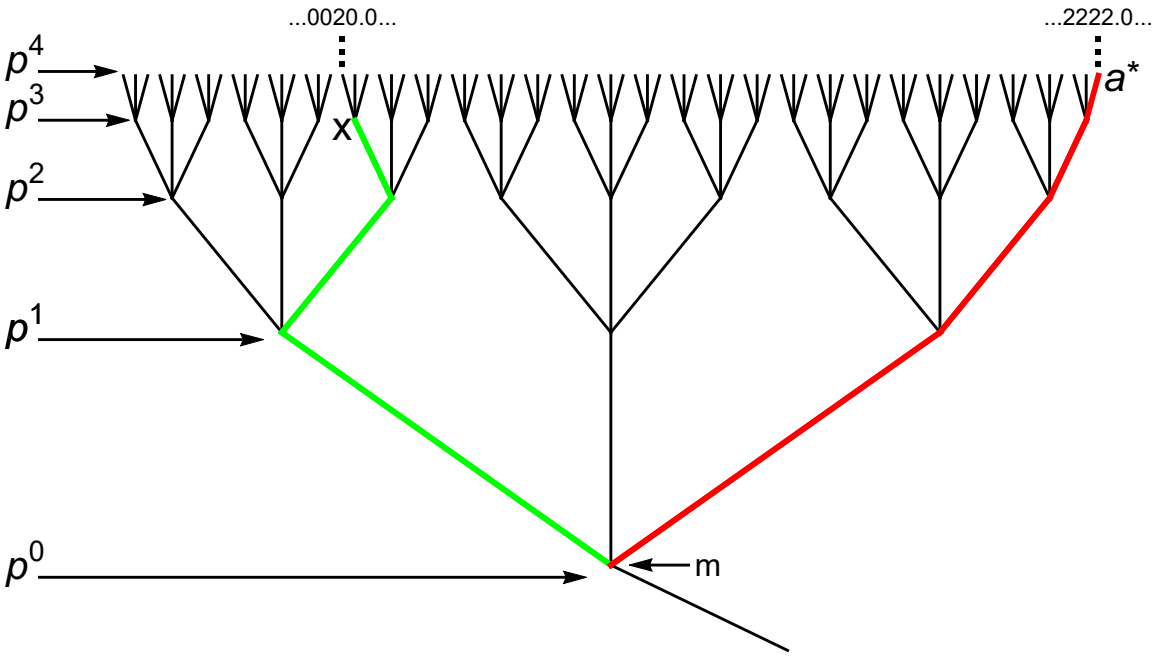

Figure 3.3: *A visual example of the second case, in which to travel from a^* to x we must travel down the tree to a point m and then back up again. There are two legs to this path, one from a^* down to m, shown in red, and one from m up to x, shown in green. We can also explicitly verify Eqn. 3.23 in this particular situation: we see by counting that there are 7 edges between a^* and x. This confirms Eqn. 3.23, as we see that* $\frac{|a_0|_p|x_0|_p}{|a_n-x_n|_p^2} = \frac{p^{-4}p^{-3}}{|2222.0-0020.0|_p^2} = \frac{p^{-7}}{(p^{-0})^2} = p^{-d_2(x,a^*)}$.

compute

$$K_\phi(x_n, x_0; a_n) = \frac{\zeta_p(2\Delta_\phi)}{p^{\Delta_\phi}} \lim_{|a_0|_p \to 0} |a_0|_p^{-\Delta_\phi} \frac{|a_0|_p^{\Delta_\phi}|x_0|_p^{\Delta_\phi}}{\sup|(x_0, a_n - x_n)|_p^{2\Delta_\phi}} \tag{3.26}$$

which simplifies to

$$K_\phi(x_n, x_0; a_n) = \frac{\zeta_p(2\Delta_\phi)}{p^{\Delta_\phi}} \frac{|x_0|_p^{\Delta_\phi}}{\sup|(x_0, a_n - x_n)|_p^{2\Delta_\phi}}. \tag{3.27}$$

This, finally is what we want: an explicit expression for K_ϕ, the bulk-to-boundary propagator for our ϕ field.

Chapter 4

Gravitons on the Tree

Until now, we have assumed that the length of all edges on the tree has been constant; we have assumed each edge has been of length 1, and so we have ignored any discussion of edge variation. However, we can consider edge length fluctuations, such that not all edges are the same length. These fluctuations in the edge lengths are like the spacetime fluctuations which result in gravity, and so we consider edge length fluctuations to be excitations of a graviton field. We represent the value of this graviton field as $J(x, y)$ which takes values on the edge between vertices x and y; note that $J(x, y)$ is only defined when $y \sim x$. Similarly to the situation with the ϕ field, we will use the shorthand $J_{xy} \equiv J(x, y)$. J_{xy} is related to the length of the edge, ℓ_{xy}, by the relationship

$$J_{xy} = \frac{1}{\ell_{xy}^2}. \tag{4.1}$$

Given this relationship, J_{xy} is like a bond strength; it becomes stronger as the lengths of the edges get smaller. In the next chapter, we will couple the J field to the ϕ field in the action through a term that is proportional to $J_{xy}(\phi_x - \phi_y)^2$. Therefore, we see that having a small edge length will increase J_{xy} and therefore increase the importance of the difference between ϕ_x and ϕ_y, which intuitively makes sense, as closer spacetime points with radically different field values should contribute to the energy more than if the points were further apart. For this chapter, however, we consider just the graviton field in the absence of matter.

For this graviton, we start with a simple Lagrangian:

$$\mathcal{L}_J = \sum_{\substack{\langle xz \rangle, \\ z \neq y}} \frac{1}{4}(J_{xy} - J_{xz})^2 + \sum_{\substack{\langle yz \rangle, \\ z \neq x}} \frac{1}{4}(J_{xy} - J_{xz})^2 + \frac{m_J^2}{2} J_{xy}^2, \tag{4.2}$$

where the first two terms are part of the kinetic term and together they sum over all edges that neighbor J_{xy}; the first term sums over those that share the endpoint x, and the second sums over all edges that share the endpoint y. Summing over all possible edges $\langle xy \rangle$, analogously to integrating over all of spacetime, we arrive at an action

$$S_J = \sum_{\langle xy \rangle} \left[\frac{1}{4} \left(\sum_{\substack{\langle xz \rangle, \\ z \neq y}} (J_{xy} - J_{xz})^2 + \sum_{\substack{\langle yz \rangle, \\ z \neq x}} (J_{xy} - J_{yz})^2 \right) + \frac{m_J^2}{2} J_{xy}^2 \right]. \tag{4.3}$$

We can also write this action in a somewhat more intuitive way by noting that, with the term inside the inner set of parentheses, a sum over all neighbors of an edge (the inner pair of sums) summed over all edges (the outer $\langle xy \rangle$ sum) is just a sum over all pairs of edges, except that we count every pair twice in the first scheme. To see this, imagine any pair of edges, $\langle uv \rangle$ and $\langle uw \rangle$. When we identify $\langle uv \rangle$ with $\langle xy \rangle$, we will have a term in the inner set of parentheses that looks like $(J_{uv} - J_{uw})^2$, and when we identify $\langle uw \rangle$ with $\langle xy \rangle$, we will have a term that looks like $(J_{uw} - J_{uv})^2$, which is the same thing; therefore, we will have two identical terms for every pair of edges. Therefore, we can rewrite our action as

$$S_J = \frac{1}{2} \sum_{\langle \langle xy \rangle \langle yz \rangle \rangle} (J_{xy} - J_{yz})^2 + \frac{1}{2} \sum_{\langle xy \rangle} m_J^2 J_{xy}^2. \tag{4.4}$$

where the notation under the first sum indicates we sum over all pairs of edges.

As with the ϕ field, to get an equation of motion, we pick a specific edge $\langle vw \rangle$ and vary the action (we will use the simpler form in Eqn. 4.3) with respect to this specific edge. This gives us the following equation of motion:

$$m_J^2 J_{xy} + \left(\sum_{\substack{\langle xz \rangle, \\ z \neq y}} (J_{xy} - J_{xz)} + \sum_{\substack{\langle yz \rangle, \\ z \neq x}} (J_{xy} - J_{yz}) \right) = 0. \tag{4.5}$$

Because J_{xy} has p neighbors on either side of it, we can pull it out of each sum and rewrite Eqn. 4.5 as

$$\left(m_J^2 + 2p\right) J_{xy} - \sum_{\substack{\langle xz \rangle, \\ z \neq y}} J_{xz} - \sum_{\substack{\langle yz \rangle, \\ z \neq x}} J_{yz}, \tag{4.6}$$

Finally, we note that we can define the edge Laplacian $\Box_e$ as

$$\Box_e J_{xy} \equiv \sum_{\substack{\langle xz\rangle,\\ z\neq y}} (J_{xy} - J_{xz}) + \sum_{\substack{\langle yz\rangle,\\ z\neq x}} (J_{xy} - J_{yz}), \tag{4.7}$$

and thus we can also write our equation of motion as

$$\Box_e J_{xy} + m_J^2 J_{xy} = 0. \tag{4.8}$$

4.1 Bulk-to-Bulk J Propagator

As with the ϕ equation of motion, we want to find a Green's function for our equation of motion, Eqn. 4.8, to serve as our propagator from one bulk point to another. We specify this Green's function by $G_J(xy, wz)$; the form of the arguments to this function indicate that it is a function of two edges, one of which is specified by two vertices x and y and the other of which is specified by two other vertices w and z. This Green's function must satisfy the equation

$$\Box_e G_J(xy, wz) + m_J^2 G_J(xy, wz) = \delta(xy, wz). \tag{4.9}$$

Written out explicitly, this means, for $\langle wz\rangle \neq \langle xy\rangle$,

$$\Box_e G_J(xy, wz) + m_J^2 G_J(xy, wz) = 0, \tag{4.10}$$

and for $\langle wz\rangle = \langle xy\rangle$,

$$\Box_e G_J(xy, xy) + m_J^2 G_J(xy, xy) = 1. \tag{4.11}$$

We start, similarly to how we started in the case of ϕ, with an ansatz of the form

$$G_J(xy, wz) = A p^{-\Delta_J d_J(xy,wz)}, \tag{4.12}$$

where $d_J(xy, wz)$ measures the distance between two edges by counting the number of vertices between them, Δ_J relates to the graviton mass and to the dimension of the corresponding operator in the related CFT, and A is a scaling constant. Plugging this ansatz

into Eqn. 4.10, we find

$$\begin{aligned} &A(p)\left(p^{-\Delta_J d_J(xy,wz)} - p^{-\Delta_J[d_J(xy,wz)+1]}\right) \\ &\quad + A\left(p^{-\Delta_J d_J(xy,wz)} - p^{-\Delta_J[d_J(xy,wz)+1]}\right) + Am_J^2 p^{-\Delta_J d_J(xy,wz)} = 0 \end{aligned} \tag{4.13}$$

$$\Rightarrow m_J^2 + p\left(1 - p^{-\Delta_J}\right) + \left(1 - p^{\Delta_J}\right) = 0 \tag{4.14}$$

$$\Rightarrow m_J^2 = -\frac{1}{\zeta_p(-\Delta_J)\zeta_p(\Delta_J - 1)}. \tag{4.15}$$

To arrive at the Eqn. 4.13, we note that there is a unique path from $\langle xy\rangle$ to $\langle wz\rangle$, and it will pass through one of the neighbors of $\langle xy\rangle$. Since we have freedom in which vertex to explicitly label as x, let us suppose the path from $\langle xy\rangle$ to $\langle wz\rangle$ passes through the vertex we label as x. Then, in addition to having the aforementioned neighbor that is one step closer to $\langle wz\rangle$, which is represented by the second term in Eqn. 4.13, the edge $\langle xy\rangle$ will also have $p-1$ other neighbors that share the vertex x, and each of these neighbors will be the same distance from $\langle wz\rangle$ as $\langle xy\rangle$ is. These do not show up in Eqn. 4.13 because they contribute nothing to our sum, since their contribution will look like $p^{-d_J(xy,wz)} - p^{-d_J(xy,wz)} = 0$. Finally, there are p neighbors that share the y vertex with $\langle xy\rangle$, represented by the first term in Eqn. 4.13; each of these edges is one more step away from $\langle wz\rangle$ than $\langle xy\rangle$ is, because we must also cross vertex y to reach them.

We can also solve for the constant A using Eqn. 4.11:

$$A(2p)\left(1 - p^{-\Delta_J}\right) - \frac{A}{\zeta_p(-\Delta_J)\zeta_p(\Delta_J - 1)} = 1 \tag{4.16}$$

$$\Rightarrow A = \frac{\zeta_p(\Delta_J)}{p^{\Delta_J} + p}. \tag{4.17}$$

Because $\langle xy\rangle$ has $2p$ neighbors, each one step away, our $\Box_e G(xy, xy)$ term looks like the first term of Eqn. 4.16. Given this, we conclude that

$$G_J(xy, wz) = \left(\frac{\zeta_p(\Delta_J)}{p^{\Delta_J} + p}\right) p^{-\Delta_J d_J(xy,wz)}. \tag{4.18}$$

Thus, in a similar vein to the scalar case, the bulk-to-bulk propagator is directly proportional to p to the power of the distance times Δ_J.

4.2 Bulk-to-Boundary J Propagator

We now want to also compute the bulk-to-boundary propagator K_J to find the propagation behavior of a graviton as it goes to the boundary of the tree. In a similar vein to what we did with the ϕ field, we will take

$$K_J(xy, ab) = \lim_{|a_0|_p \to 0} |a_0|^{-\Delta_J} G(xy, a^* b^*), \tag{4.19}$$

where again, letters from the end of the alphabet represent bulk vertices, letters from the beginning of the alphabet represent edge points, and a^* and b^* represent bulk points related to the p-adic numbers a_n and b_n respectively, and with finite depths a_0 and b_0, such that $\langle a^* b^* \rangle \to \langle ab \rangle$ as $|a_0|_p \to 0$. We also assume that the earlier letter of a pair is the higher of the two vertices in the tree (e.g. a is higher than b, a^* is higher than b^*, x is higher than y, etc.). However, we cannot proceed with taking this limit until we have a more explicit expression for the distance between two edges, so it is to this that we now turn.

4.2.1 Distance Between Edges

As mentioned at the end of Section 2.2, we can associate a depth with each edge that is the same as the depth of its upper vertex (the vertex closer to the p-adic boundary of the tree). We will make use of this convention in this section. To begin, we assume that $\langle a^* b^* \rangle$ is higher or at the same height as $\langle xy \rangle$, or mathematically, $|a_0|_p \leq |x_0|_p$. As before, we have two cases; either the path from a^* to the point at ∞ passes through x (and therefore the edge $\langle xy \rangle$), or it does not. An example of the first situation is represented in Fig. 4.1 and example of the second is shown in Fig. 4.2.

In the first case, the path from one edge to the other is a "straight shot." Thus we merely have to count the number of vertices we cross in going down from the higher edge to the lower, which is

$$p^{-d_1(xy, a^* b^*)} = \frac{|a_0|_p}{|x_0|_p}. \tag{4.20}$$

This is the same formula as Eqn. 3.22, and this works because for every edge that we count in determining the distance from a^* to x, there is a vertex at the end of that edge that we would also like to count towards our distance between the edges $\langle a^* b^* \rangle$ and $\langle xy \rangle$. A visual representation of this situation is presented in Fig. 4.1.

In the second case, we must descend from $\langle a^* b^* \rangle$ to a "common ancestor" vertex, which we will label as m, and then ascend again to $\langle xy \rangle$. There will be two edges at the level just

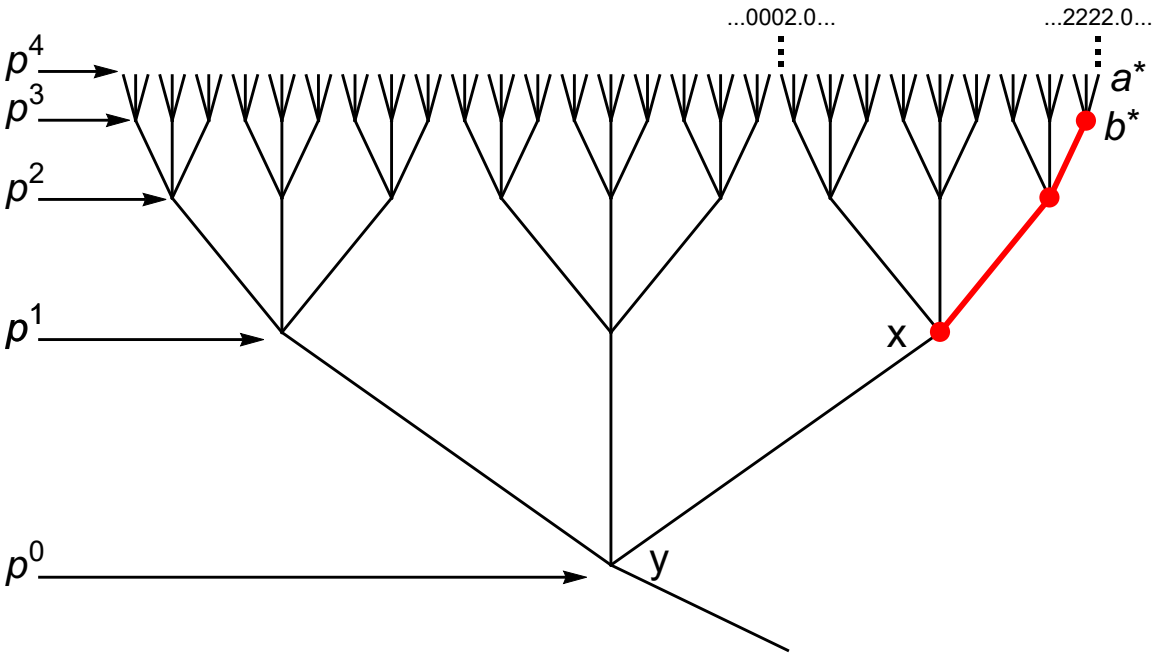

Figure 4.1: *An example of the first case, in which $\langle xy\rangle$ is on the path from $\langle a^*b^*\rangle$ to ∞. We can use this diagram to show that Eqn. 4.20 holds in this example. We see the number of vertices between $\langle a^*b^*\rangle$ and $\langle xy\rangle$ is 3 (as indicated by the red dots), and we see that this agrees with Eqn. 4.20:* $\frac{|a_0|_p}{|x_0|_p} = \frac{p^{-4}}{p^{-1}} = p^{-3} = p^{-d_1(xy,a^*b^*)}$.

above our lowest common vertex, one on the branch towards $\langle a^*b^*\rangle$ and the other on the $\langle xy\rangle$ branch. Let us call these edges $\langle cm\rangle$ and $\langle mw\rangle$ respectively, noting that c and w are both higher than m; see Fig. 4.2 for a visualization. We see that the number of vertices crossed in going from $\langle a^*b^*\rangle$ to $\langle cm\rangle$ is given by

$$p^{-d_2(cm,a^*b^*)} = \frac{|a_0|_p}{|c_0|_p}; \tag{4.21}$$

similarly, the distance from $\langle xy\rangle$ to $\langle mw\rangle$ is given by

$$p^{-d_2(xy,mw)} = \frac{|x_0|_p}{|w_0|_p}. \tag{4.22}$$

Our total distance from $\langle xy\rangle$ to $\langle a^*b^*\rangle$ will be the sum of $d_2(xy,mw)$ and $d_2(cm,a^*b^*)$, plus 1 because we cross a vertex when switching from $\langle cm\rangle$ to $\langle mw\rangle$. Thus we find

$$p^{-d_2(xy,a^*b^*)} = p^{-1}\frac{|a_0|_p|x_0|_p}{|c_0|_p^2}. \tag{4.23}$$

Since m is the vertex at which the path from $\langle a^*b^* \rangle$ to $\langle xy \rangle$ reaches its lowest, we should be able to represent its depth by specifying the depth of the difference between a_n and x_n, in exactly the same way as in the previous chapter: $|a_n - x_n|_p$. However, c (and w) is one step higher than m, so $|c_0|_p = |w_0|_p = p^{-1}|a_n - x_n|_p$. Plugging this in, we find

$$p^{-d_2(xy,a^*b^*)} = p\frac{|a_0|_p|x_0|_p}{|a_n - x_n|_p^2}. \tag{4.24}$$

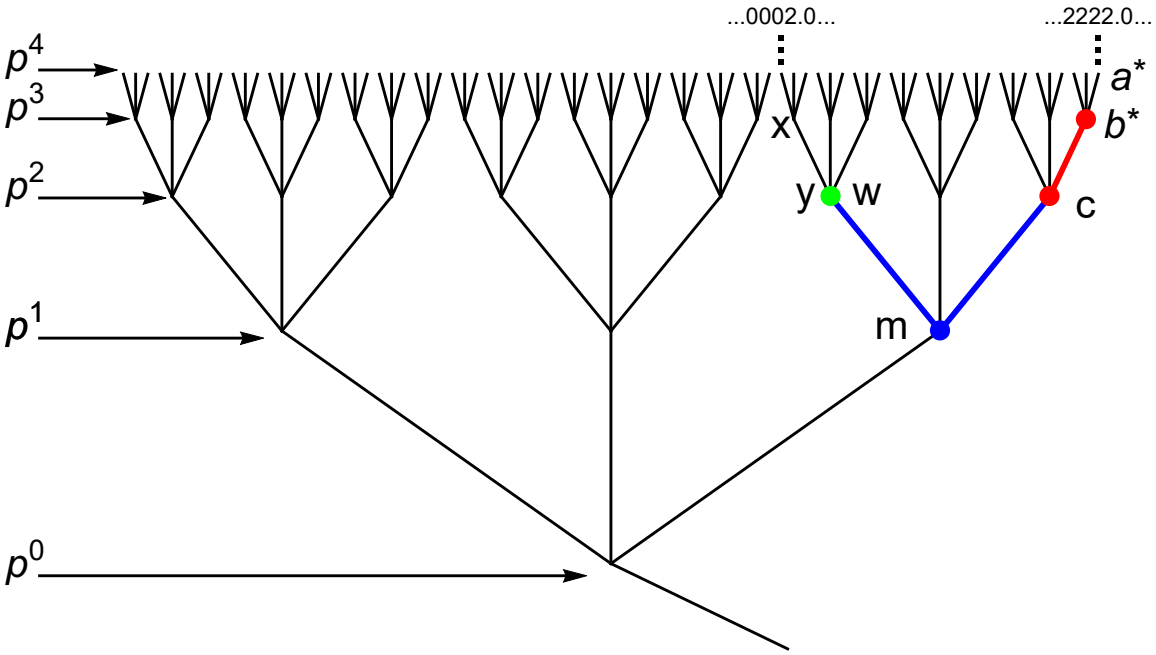

Figure 4.2: *An example of the second case, in which to travel from $\langle a^*b^* \rangle$ to $\langle xy \rangle$, we must go down to a common ancestor and then back up. We break this path into 3 segments: the red dots mark the path from $\langle a^*b^* \rangle$ to one lowest edge (the right blue edge), the green dot marks the path from $\langle xy \rangle$ to the other lowest edge (the left blue edge), and the blue dot marks the path from one lowest edge to the other. The points labeled c, m, and w are labeled appropriately following the reasoning given in the text above to derive Eqn. 4.24; note that although w and y here are the same point, this is not generally true. We can explicitly see that Eqn. 4.24 holds on this diagram, because we see that the number of vertices we must cross to get from $\langle ab \rangle$ to $\langle xy \rangle$ is 4. Working out the right hand side of Eqn. 4.24, we see agreement:* $p\frac{|a_0|_p|x_0|_p}{|a_n - x_n|_p^2} = p\frac{p^{-4}p^{-3}}{|2222.0-0002.0|_p^2} = p\frac{p^{-7}}{(p^{-1})^2} = p^{-4} = p^{-d_2(xy,a^*b^*)}$.

To mathematically distinguish the two situations described above, as before, we compare $|a_n - x_n|_p$ with $|x_0|_p$. If $|x_0|_p \geq |a_n - x_n|_p$, x must be lower than or at the same level as the common ancestor m, and so $\langle xy \rangle$ must be on the path from $\langle a^*b^* \rangle$ to ∞, so therefore we are in situation 1; otherwise, we are in situation 2. Furthermore, if we are in situation

1, $|x_0|_p^2 \geq |a_n - x_n|_p^2$ which in turn means that $|x_0|_p^2 > \frac{|a_n - x_n|_p^2}{p}$.

Some examples may help to clarify this: for example, in Fig. 4.1, which represents situation 1, $|x_0|_p^2 = \left(p^{-1}\right)^2$ and $\frac{|a_n - x_n|_p^2}{p} = \frac{|2222.0 - 0002.0|_p^2}{p} = p^{-3}$, so therefore $|x_0|_p^2 > \frac{|a_n - x_n|_p^2}{p}$. In Fig. 4.2, however, which represents situation 2, we see that $|x_0|_p^2 = \left(p^{-3}\right)^2$ and $\frac{|a_n - x_n|_p^2}{p} = \frac{|2222.0 - 0002.0|_p^2}{p} = p^{-3}$, so therefore $|x_0|_p^2 < \frac{|a_n - x_n|_p^2}{p}$. We can thus combine our two cases using the supremum norm:

$$p^{-d_J(xy,a^*b^*)} = |a_0|_p \begin{cases} \frac{p|x_0|_p}{|a_n - x_n|_p^2} & |a_n - x_n|_p \geq |x_0|_p \\ \frac{1}{|x_0|_p} & |a_n - x_n|_p < |x_0|_p. \end{cases} \tag{4.25}$$

$$\Rightarrow p^{-d_J(xy,a^*b^*)} = \frac{|x_0|_p |a_0|_p}{\sup\left(\frac{|a_n - x_n|_p^2}{p}, |x_0|_p^2\right)}. \tag{4.26}$$

We can now use this result to express our bulk-to-bulk propagator more explicitly:

$$G_J(xy, a^*b^*) = \left(\frac{\zeta_p(\Delta_J)}{p^{\Delta_J} + p}\right) \frac{|x_0|_p^{\Delta_J} |a_0|_p^{\Delta_J}}{\sup\left(\frac{|a_n - x_n|_p^2}{p}, |x_0|_p^2\right)^{\Delta_J}}. \tag{4.27}$$

Now, finally, we are ready to calculate the bulk-to-boundary propagator. Using Eqn. 4.19 to take $\langle a^*b^* \rangle$ to the edge of the tree (where it becomes $\langle ab \rangle$), we find

$$K_J(xy, ab) = \lim_{|a_0|_p \to 0} |a_0|_p^{-\Delta_J} \left(\frac{\zeta_p(\Delta_J)}{p^{\Delta_J} + p}\right) \frac{|x_0|_p^{\Delta_J} |a_0|_p^{\Delta_J}}{\sup\left(\frac{|a_n - x_n|_p^2}{p}, |x_0|_p^2\right)^{\Delta_J}} \tag{4.28}$$

$$\Rightarrow K_J(xy, ab) = \left(\frac{\zeta_p(\Delta_J)}{p^{\Delta_J} + p}\right) \frac{|x_0|_p^{\Delta_J}}{\sup\left(\frac{|a_n - x_n|_p^2}{p}, |x_0|_p^2\right)^{\Delta_J}}. \tag{4.29}$$

Thus, we have found an explicit expression for the bulk-to boundary propagator for the graviton, written in terms of the bulk edge depth and the p-adic numbers associated with each edge.

Chapter 5

General Relativity on the Tree

So far, we have considered the scalar ϕ field and the graviton J field independently; in this chapter, however, we wish to consider both of them together and how they might interact in an Einstein-like theory of gravity.

The Einstein equation in ordinary Minkowski space, which is the foundation of general relativity calculations and which will serve as our general guide in this chapter, is

$$R_{\mu\nu} - \frac{1}{2}Rg_{\mu\nu} + \Lambda g_{\mu\nu} = 8\pi T_{\mu\nu} \tag{5.1}$$

Schematically, the left hand side of this equation describes the curvature of spacetime, given by a combination of the trace of the Ricci tensor, $R_{\mu\nu}$, the metric, $g_{\mu\nu}$, the Ricci scalar R, and the cosmological constant Λ. The right hand describes the matter distribution in the space given by the stress-energy tensor, $T_{\mu\nu}$. Ideally, we would like to formulate this equation on our Bruhat-Tits tree, using notation and operations appropriate to the fact that we are working on a tree lattice and not a continuum. At first glance this seems rather difficult to do, as the concept of "curvature" and even the Christoffel symbols from which the Ricci tensor is often constructed do not have a clear analogue for the tree.

5.1 The Einstein Equation Without Matter

Despite the lack of obvious ways to construction $R_{\mu\nu}$ on the Bruhat-Tits tree, Gubser et al. realized that they could exploit a relationship between the trace of the Ricci tensor, $R_{\mu\nu}$, and the notion of transport distance $W(B_0(x), B_0(y))$ [1]. Using a defintion of W on the Bruhat-Tits lattice, they were able to construct an equivalent for the left hand side of the Einstein equation, which when set equal to 0 is a full Einstein equation when no matter is

present ($T_{\mu\nu} = 0$).

In the conventional sense of transport distance, if x and y are points in a space, W measures the weighted average of distances between points in a small ball of radius a around x (which we denote $B_0(x)$) and points in a small ball of radius a around y (which we denote as $B_0(y)$). Then, up to some multiplicative constants, the Ricci tensor $R_{\mu\nu}$ can be written as

$$R_{\mu\nu} \propto \frac{1}{a^2}\left(1 - \frac{W(B_0(x), B_0(y))}{d(x,y)}\right) \tag{5.2}$$

where $d(x,y)$ measures the distance between the points x and y. However, on a lattice, the concept of a "small ball" around a vertex makes no sense, since if $a < \ell$ (where ℓ is the lattice spacing), there is only one point in our ball. Instead, Gubser et al. imagined that we associate a probability distribution $\psi_x(t)$ with every vertex x, with most of the probability on x, but a small amount of probability, proportional to the small number t, at each neighbor. Therefore, if we pick vertices from this probability distribution, the average distance from x will be small (less than an edge length), but non-zero. We can therefore define a weighted average distance between points in two neighboring probability distributions, $\psi_x(t)$ and $\psi_y(t)$, and we can use that as our transport distance. Assuming t is small (and indeed they eventually take the limit $t \to 0$), Gubser et al. define the equivalent of the trace of the Ricci tensor, which they denote as κ_{xy}, for a pair of vertices x and y, in analogue to Eqn. 5.2:

$$\kappa_{xy} = \lim_{t\to 0}\frac{1}{t}\left(1 - \frac{W(\psi_x(t), \psi_y(t))}{d(x,y)}\right). \tag{5.3}$$

Working out this calculation explicitly on the Bruhat-Tits tree, they find that

$$\kappa_{xy} = \frac{\sqrt{J_{xy}}}{\sum_i J_{xx_i}}\left(2\sqrt{J_{xy}} - \sum_i \sqrt{J_{xx_i}}\right) + \frac{\sqrt{J_{xy}}}{\sum_i J_{yy_i}}\left(2\sqrt{J_{xy}} - \sum_i \sqrt{J_{yy_i}}\right), \tag{5.4}$$

where the notation x_i indicates a vertex that is a neighbor of x (here that includes y; note this convention differs slightly from that in Gubser et al.), and a sum over all i of J_{xx_i} indicates a sum over all edges that have x as an endpoint. This presentation of κ_{xy} was somewhat schematic, and readers interested in a more detailed derivation are encouraged to look at Section 3 of Gubser's paper [1].

Since we can derive the matter-free equations of motion for gravity in ordinary Minkowski space from the Einstein-Hilbert action, given by

$$S_H = \int [R - 2\Lambda]\sqrt{-g}d^4x \tag{5.5}$$

by varying this action with respect to the metric $g_{\mu\nu}$, we would like to construct an equivalent of the Einstein-Hilbert action on the tree, which we will then vary. Therefore, Gubser et al. postulated that we can construct an analagous action on the tree that takes the form

$$S_G = \sum_{\langle xy \rangle} (\kappa_{xy} - 2\Lambda), \tag{5.6}$$

or, written more explicitly,

$$\begin{aligned} S_G = \sum_{\langle xy \rangle} \Bigg[& \frac{\sqrt{J_{xy}}}{\sum_i J_{xx_i}} \left(2\sqrt{J_{xy}} - \sum_i \sqrt{J_{xx_i}} \right) \\ & + \frac{\sqrt{J_{xy}}}{\sum_i J_{yy_i}} \left(2\sqrt{J_{xy}} - \sum_i \sqrt{J_{yy_i}} \right) - 2\Lambda \Bigg], \end{aligned} \tag{5.7}$$

where the sum over all edges is thought to achieve the same thing as tracing over $R_{\mu\nu}$ and integrating over all of spacetime.

In this thesis, we will be considering solutions to our equations of motion that involve fields that deviate only slightly from some static background field configuration. If we consider J_{xy} to be only slightly perturbed from a uniform background value of 1 (meaning the edge lengths throughout the entire tree will fluctuate only slightly away from length 1), this means we can write our J_{xy} values as

$$J_{xy} = 1 + j_{xy} \tag{5.8}$$

where $\text{abs}(j_{xy}) \ll 1$. If we make this substitution into Eqn. 5.7, we find that we recover the action given by Eqn. 4.3 for $m_J = 0$ (which makes sense as we want gravitons to be massless). For an explicit demonstration of this equivalence, see Appendix A. Therefore, we see that the work we have done previously with gravitons is applicable to this theory too if we are working in the regime in which $\text{abs}(J_{xy} - 1) \ll 1$.

Having thus motivated how our previous discussions relate to the current discussion of general relativity on the tree, we now turn to actually formulating an Einstein equation on the tree. As noted previously, one way of obtaining the Einstein general relativity equations is to vary the Einstein-Hilbert action, Eqn. 5.5, with respect to $g_{\mu\nu}$; in the absence of matter, this will in give us

$$\delta S_H = \sqrt{-g} \left(R_{\mu\nu} - \frac{1}{2} R g_{\mu\nu} \right) \delta g^{\mu\nu} = 0. \tag{5.9}$$

Gubser et al. similarly take their action for the tree (Eqn. 5.7) and vary it, here with

respect to J_{xy}, and they show that this variation, divided by δJ_{xy}, gives us the equivalent of the left hand side of the Einstein equation. For a detailed look at exactly how this was done, the reader is encouraged to read Section 3.2 of their paper [1]. The result of taking $\frac{\delta S_G}{\delta J_{xy}}$ and setting it equal to 0, giving the Einstein equation on the tree with no matter, is

$$\sqrt{J_{xy}}\frac{\left(\sum_i \sqrt{J_{xx_i}}\right)^2}{\left(\sum_i J_{xx_i}\right)^2} - \frac{\sum_i \sqrt{J_{xx_i}}}{\sum_i J_{xx_i}} + \sqrt{J_{xy}}\frac{\left(\sum_i \sqrt{J_{yy_i}}\right)^2}{\left(\sum_i J_{yy_i}\right)^2} - \frac{\sum_i \sqrt{J_{yy_i}}}{\sum_i J_{yy_i}} = 0. \tag{5.10}$$

5.2 The Einstein Equation With Matter

In this thesis, we would like to find the more general Einstein equation that includes terms relating to matter, which will schematically result in the right hand side of Eqn. 5.10 becoming non-zero. As with finding the left hand side of the Einstein equation, we ultimately turn to variations of the action to provide us with the correct representation of the right hand side of the equation on the tree. First, however, we must start with an action that includes matter. We posit that the part of the action involving matter, S_M, will look like

$$S_M = \sum_{\langle xy \rangle} \frac{J_{xy}}{2}(\phi_x - \phi_y)^2 + \sum_x V(\phi_x), \tag{5.11}$$

where $V(\phi_x)$ is some potential that is a purely local function of ϕ. The first term in this action, the kinetic term, couples to the graviton field in a natural way, because as mentioned in Chapter 4 this coupling means that a shorter edge puts greater weight (larger J_{xy}) on the difference between the ϕ fields at two close vertices. We thus add this to the curvature action, Eqn. 5.7, to get our total action,

$$S_{\text{tot}} = \sum_{\langle xy \rangle} (\kappa_{xy} - 2\Lambda) + \sum_{\langle xy \rangle} \frac{J_{xy}}{2}(\phi_x - \phi_y)^2 + \sum_x V(\phi_x). \tag{5.12}$$

Since we previously used the fact that the variation of S_G is 0 when there is no matter, and from that derived the matter-free Einstein equation on the tree, we now set the variation of $S_{\text{tot}} = 0$ to find the Einstein equation with matter. Since we can easily see that

$$\frac{\delta S_M}{\delta J_{xy}} = \frac{1}{2}(\phi_x - \phi_y)^2 \tag{5.13}$$

and since $\frac{\delta S_{\text{tot}}}{\delta J_{xy}} = 0$ implies that $\frac{\delta S_G}{\delta J_{xy}} = -\frac{\delta S_M}{\delta J_{xy}}$, we conclude that our total Einstein equation

should be

$$\sqrt{J_{xy}}\frac{\left(\sum_i \sqrt{J_{xx_i}}\right)^2}{\left(\sum_i J_{xx_i}\right)^2} - \frac{\sum_i \sqrt{J_{xx_i}}}{\sum_i J_{xx_i}} + \sqrt{J_{xy}}\frac{\left(\sum_i \sqrt{J_{yy_i}}\right)^2}{\left(\sum_i J_{yy_i}\right)^2} - \frac{\sum_i \sqrt{J_{yy_i}}}{\sum_i J_{yy_i}} = -\frac{1}{2}(\phi_x - \phi_y)^2. \tag{5.14}$$

This equation will serve as one of our primary equations of motion as we try in the next chapter to find solutions for J and ϕ fields together on the tree. The other equation can be obtained by varying the action S_{tot} as given in Eqn. 5.12 with respect to ϕ_x. This will then give us

$$\sum_{y\sim x} J_{xy}(\phi_x - \phi_y) = -\frac{\partial V(\phi_x)}{\partial \phi_x}, \tag{5.15}$$

which is our Klein-Gordon equation for ϕ and will serve as our second equation of motion.

Chapter 6

Gravity-Matter Solutions on the Tree

Having established the equations of motion for particles on the tree, we would now like to solve them. The entire field of possible solutions is vast, and we will not attempt to discover all of them. Rather, we will restrict ourselves only to solutions with certain symmetry properties, which will both simplify our job computationally and will be more natural and intuitive than a random solution.

6.1 Depth-Dependent Solution

First, let us assume that the values of ϕ and J depend only on their depth in the tree, which is to say all edges at the same "level" in the tree have the same value as each other, and all vertices at the same level have the same value; see Fig. 6.1 for a visual representation.

To simplify notation, we let $J_{xy} = b_{xy}^2$, so that we can deal with equations involving integer powers of b instead of half-integer powers of J. With this, along with the assumption that values depend only on the depth in a tree, we can choose any vertex level and call that level i, with all vertices at that level having a value that we call ϕ_i. Similarly, we can label the edges immediately below those vertices as also at level i, and each edge at this depth will have length $\frac{1}{\sqrt{J_i}} = \frac{1}{b_i}$ (see Eqn. 4.1). We will also find ϕ_{i-1}, ϕ_{i+1}, b_{i-1}, and b_{i+1} useful in our discussion, where a subscript of $i-1$ indicates an edge or vertex immediately above the i level, while a subscript of $i+1$ indicates the vertex or edge level just below the i level. Consequently, infinitely far up the tree, at the boundary with the p-adic numbers, $i = -\infty$, while infinitely far down the tree, at the point at infinity, $i = \infty$. In a sense, these values

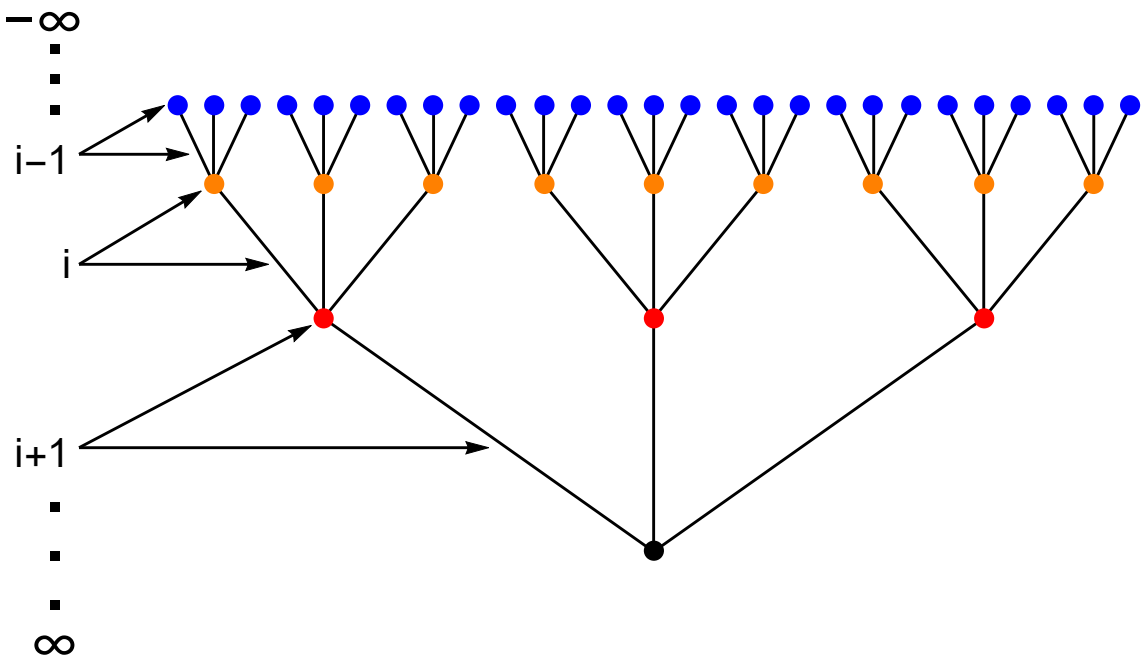

Figure 6.1: *On this p=3 tree, the vertices are colored corresponding to their values, indicating which vertices have the same value as others; we see that the values are determined by depth in the tree. The same principle holds for the edges, which we did not explicitly color, but the edges between the same sets of colors all have the same length; for example, all the edges that have one orange vertex and one red vertex are all the same length. On the left, we demonstrate our labeling scheme, by setting edges and vertices higher in the tree to be labeled by a more negative number and those lower in the tree to be labeled by a larger positive number. Note that edge lengths are drawn for aesthetic convenience, not with correct relative lengths to each other.*

of i represent the distance from the top of the tree, offset by an infinite constant. This labeling scheme is demonstrated in Fig. 6.1.

With this notation, we can write our second equation of motion, Eqn. 5.15, by realizing that for any given vertex, it will have p neighbors at the level above it (at level $i-1$) and one neighbor at the level below it (at level $i+1$). Therefore, we can split the sum in Eqn. 5.15 into

$$pb_{i-1}^2\left(\phi_i-\phi_{i-1}\right)+b_i^2\left(\phi_i-\phi_{i+1}\right)=-\frac{\partial V(\phi_i)}{\partial\phi_i} \tag{6.1}$$

and we can expand the sums from Eqn. 5.14 in a similar fashion to obtain an Einstein equation of

$$b_i\frac{\left(pb_{i-1}+b_i\right)^2}{\left(pb_{i-1}^2+b_i^2\right)^2}-\frac{pb_{i-1}+b_i}{pb_{i-1}^2+b_i^2}+b_i\frac{\left(pb_i+b_{i+1}\right)^2}{\left(pb_i^2+b_{i+1}^2\right)^2}-\frac{pb_i+b_{i+1}}{pb_i^2+b_{i+1}^2}=-\frac{1}{2}\left(\phi_i-\phi_{i+1}\right)^2 \tag{6.2}$$

We can multiply this second equation by a factor of $(pb_{i-1}^2 + b_i^2)^2(pb_i^2 + b_{i+1}^2)^2$ in order to eliminate all denominators (this is valid as we never expect any edge lengths to be negative or 0, so the quantity we multiply by is never 0). Thus, Eqn. 6.2 becomes

$$\begin{aligned}\left[(p^2-p)b_i b_{i-1}^2 + pb_i^2 b_{i-1} - p^2 b_{i-1}^3\right](pb_i^2 + b_{i+1}^2)^2 \\ + \left[(1-p)b_i b_{i+1}^2 + pb_i^2 b_{i+1} - b_{i+1}^3\right](pb_{i-1}^2 + b_i^2)^2 \\ = -\frac{1}{2}(\phi_i - \phi_{i+1})^2(pb_{i-1}^2 + b_i^2)^2(pb_i^2 + b_{i+1}^2)^2\end{aligned} \tag{6.3}$$

Rather than trying to solve this equation directly, we note that as we approach the upper boundary of the tree, we would like for the matter field to take increasingly small values. Similarly, we would like for the tree to tend towards constant negative curvature; that is, we would like for the edge lengths to tend towards 1 (this corresponds to negative curvature because the cosmological constant makes the overall curvature negative when all $J_{xy} = 1$). In other words, we would like, as i approaches $-\infty$, for the solution we get to match the trivial solution, where $\phi_i = \phi_{i-1} = \phi_{i+1} = 0$ and $b_i = b_{i-1} = b_{i+1} = 1$ for all i (the reader can check that these solutions indeed satisfy Eqns. 6.1 and 6.3 fairly trivially if $\left.\frac{\partial V(x)}{\partial x}\right|_{x=0} = 0$). In this regime, then, we can work with perturbation theory, assuming that we perturb around a background of $\phi_x = 0$ and $b_{xy} = 1$. To express this rigorously, we say that ϕ_x is of order λ, where λ is some small parameter; specifically, let us say that

$$\phi_x = \lambda\tilde{\phi}_x. \tag{6.4}$$

An order-λ perturbation in ϕ will cause an order-λ^2 perturbation in b; to see this, note that in Eqn. 6.3, the right hand side will be proportional to $(\lambda\tilde{\phi}_i - \lambda\tilde{\phi}_{i+1})^2 \sim \lambda^2$. Therefore, the lowest-order corrections to the left hand side must also be of order λ^2, indicating that fluctuations in b_{xy} must be also of order λ^2. Therefore, we can write

$$b_{xy} = 1 + \lambda^2\tilde{b}_{xy}. \tag{6.5}$$

We now return to Eqn. 6.3 and expand it in powers of λ. The zeroth-order is trivially 0, as the first multiplicative factor in each line is 0 at order λ^0. Our lowest-order non-trivial equation, then, will come when we take the order-λ^2 part of the first terms of each line, and multiply by the order-λ^0 contributions from the other multiplicative factors on each line.

Thefore at order λ^2, we find

$$\begin{aligned}\left[(p^2-p)\lambda^2\tilde{b_i}+2(p^2-p)\lambda^2\tilde{b}_{i-1}+2p\lambda^2\tilde{b_i}+p\lambda^2\tilde{b}_{i-1}-3p^2\lambda^2\tilde{b}_{i-1}\right](p+1)^2 \\ +\left[(1-p)\lambda^2\tilde{b_i}+2(1-p)\lambda^2\tilde{b}_{i+1}+2p\lambda^2\tilde{b_i}+p\lambda^2\tilde{b}_{i+1}-3\lambda^2\tilde{b}_{i+1}\right](p+1)^2 \\ =-\frac{1}{2}\lambda^2(\tilde{\phi_i}-\tilde{\phi}_{i+1})^2(p+1)^2(p+1)^2\end{aligned} \tag{6.6}$$

Cancelling a factor of $(p+1)^2$ in every term and combining terms inside the brackets, this simplifies to

$$(p^2+2p+1)\tilde{b_i}-(p^2+p)\tilde{b}_{i-1}-(p+1)\tilde{b}_{i+1}=-\frac{1}{2}(\tilde{\phi_i}-\tilde{\phi}_{i+1})^2(p+1)^2 \tag{6.7}$$

Using the perturbation assumptions given in Eqns. 6.4 and 6.5, we can also expand Eqn. 6.1 in powers of λ. The first non-trivial equation in this expansion is of order λ:

$$p(\tilde{\phi_i}-\tilde{\phi}_{i-1})+\tilde{\phi_i}-\tilde{\phi}_{i+1}=-\left.\frac{\partial^2 V(\phi_i)}{\partial\phi_i^2}\right|_{\phi_i=0}\tilde{\phi_i}. \tag{6.8}$$

This is a particularly nice result if we assume $V(\phi_x)$ is a function that can be expanded as a MacLaurin series about $\phi_x=0$, because it means that the right hand side of Eqn. 6.8 merely picks out the coefficient of the term of V that is quadratic in ϕ_x; the rest either disappear because of the derivatives or vanish when we set $\phi_i=0$. Therefore, we assume now that $V(\phi_i)=r\phi_i^2$, where r is some constant value (which could be 0). This expression for the potential may have large corrections at other orders of ϕ_x (and therefore λ), but we ignore those as they are irrelevant for the discussion here, since we are dealing only with order-λ terms.

Now we can write our difference equations: substituting r into Eqn. 6.8 and rearranging, we find

$$\tilde{\phi}_{i+1}-(p+1+r)\tilde{\phi_i}+p\tilde{\phi}_{i-1}=0 \tag{6.9}$$

and simplifying Eqn. 6.7, we get

$$\tilde{b}_{i+1}-(p+1)\tilde{b_i}+p\tilde{b}_{i-1}=\frac{1}{2}(\tilde{\phi_i}-\tilde{\phi}_{i+1})^2(p+1) \tag{6.10}$$

Eqn. 6.9 appears to be the easier equation to solve, so we begin there. This is a second-order homogeneous difference equation, so we can solve it by assuming an ansatz of the form

$$\tilde{\phi}_n=A\alpha^n \tag{6.11}$$

for some numbers A and α. Plugging this ansatz into Eqn. 6.9 and simplifying, we find

$$\alpha^2 - (p+1+r)\alpha + p = 0, \tag{6.12}$$

which has solutions of the form

$$\alpha_{1,2} = \frac{p+1+r \pm \sqrt{(p+1+r)^2 - 4p}}{2} \tag{6.13}$$

We can write this in a more illuminating form if we parametrize r by saying that

$$r = -p - 1 \pm \left(p^{\Delta_\phi} + p^{-\Delta_\phi+1}\right), \tag{6.14}$$

which we note is consistent with Eqn. 3.15 if we take $r = m_\phi^2$ (as the coefficient of the ϕ^2 term in the action), and if we take the plus sign in Eqn. 6.14. Since we assume that Δ_ϕ can take any real value, we have not restricted r in any way by specifying this parametrization except by requiring that either $r \geq -p-1+2\sqrt{p}$ or $r \leq -p-1-2\sqrt{p}$, which we see is what is already required of r to make the solutions α_1 and α_2 real. Using this, we can rewrite $\alpha_{1,2}$ rather nicely:

$$\alpha_{1,2} = \frac{\pm\left(p^{\Delta_\phi} + p^{-\Delta_\phi+1}\right) \pm \left(p^{\Delta_\phi} - p^{-\Delta_\phi+1}\right)}{2} \tag{6.15}$$

and therefore we say

$$\alpha_1 = \pm p^{\Delta_\phi}; \qquad \alpha_2 = \pm p^{-\Delta_\phi+1}, \tag{6.16}$$

where we note that either both α's are positive or both are negative, since the first $\pm$ is set by the value of r which will be consistent between both α's. Thus, in general we find that

$$\tilde{\phi}_i = A_1(\pm 1)^i p^{\Delta_\phi i} + A_2(\pm 1)^i p^{(-\Delta_\phi+1)i}, \tag{6.17}$$

or more schematically,

$$\tilde{\phi}_i = A_1\alpha_1^i + A_2\alpha_2^i, \tag{6.18}$$

for arbitrary constants A_1 and A_2. However, we would like our ϕ field to vanish as we move further up in the tree (i becomes more negative), so we set $A_2 = 0$ if $\Delta_\phi > 1$ and we set $A_1 = 0$ if $\Delta_\phi < 0$.

We also note that p^n is merely the reciprocal of the depth of a point in the tree, and

therefore we can replace p^n with $|x_0|_p$, where the depth x_0 corresponds to the level n. We note that by stepping down the tree by one step, p^n increases by a factor of p, and $|x_0|_p$ also increases by a factor of p, suggesting that we have made the correct replacement. Therefore, we conclude that we can alternatively write the plus-sign solutions from Eqn. 6.17 as

$$\tilde{\phi}_x = A_1|x_0|_p^{\Delta_\phi} + A_2|x_0|_p^{-\Delta_\phi+1}. \tag{6.19}$$

Although we can have a consistent solution for any Δ_ϕ, we are particularly interested in solutions in which both α_1 and α_2 have magnitudes greater than 1, so that when we send $i \to -\infty$, $\tilde{\phi}_i$ will approach 0 even when A_1 and A_2 are both non-zero. From our remarks after Eqn. 6.18, this happens only when

$$0 < \Delta_\phi < 1. \tag{6.20}$$

We now move on to trying to solve Eqn. 6.10. Using our results from Eqn. 6.18, we must solve the equation

$$\begin{aligned}\tilde{b}_{i+1} - (p+1)\tilde{b}_i + p\tilde{b}_{i-1} = \frac{1}{2}(p+1)\Big[&A_1^2\alpha_1^{2i}(1-\alpha_1)^2 + A_2^2\alpha_2^{2i}(1-\alpha_2)^2 \\ &+ 2A_1A_2\alpha_1^i\alpha_2^i(1-\alpha_1)(1-\alpha_2)\Big]\end{aligned} \tag{6.21}$$

This is an inhomogeneous difference equation. Solving the homogeneous equation related to this is fairly straightforward: we postulate that a solution to the homogeneous equation

$$\tilde{b}_{i+1} - (p+1)\tilde{b}_i + p\tilde{b}_{i-1} = 0 \tag{6.22}$$

has the form

$$\tilde{b}_i = C\omega^i \tag{6.23}$$

which then implies, by plugging in this ansatz, that

$$\omega^2 - (p+1)\omega + p = 0, \tag{6.24}$$

which simply has the solutions

$$\omega_1 = p; \qquad \omega_2 = 1 \tag{6.25}$$

Similarly to in the case with ϕ, we would like for these solutions for the graviton field perturbation to be of the form p^{Δ_J} and $p^{-\Delta_J+1}$. If we say that $m_J^2 = 0$, as we expect our

gravitons to be massless, then from Eqn. 4.15, we see that this implies that $\Delta_J = 0$ or $\Delta_J = 1$; either of these choices leads us to conclude that the solutions to our difference equation should be proportional to p^1 and p^0, which is exactly what we see in Eqn. 6.25. However, since we want our solution to fall off high up in the tree, we reject ω_2 and will only concern ourselves with ω_1.

Our inhomogeneous solution is a bit more complicated. To find it, we break up the term on the right hand side of Eqn. 6.21 into three parts, proportional to α_1^{2i}, α_2^{2i}, and $\alpha_1^i \alpha_2^i$ respectively. We solve the inhomogeneous equation for each of these terms separately, and our total inhomogeneous solutions will simply be a sum of these partial solutions. For the terms proportional to α_1^{2i} and α_2^{2i}, we postulate that $\tilde{b}_i$ has the form

$$\tilde{b}_i = B_j \alpha_j^{2i}, \tag{6.26}$$

where $j = 1$ or 2 depending on which case we wish to consider. Then we can write our inhomogeneous equation, taking one of the α_j^{2i} terms as our right hand side, as

$$B_j \alpha_j^{2i+2} - B_j(p+1)\alpha_j^{2i} + B_j p \alpha_j^{2i-2} = \frac{1}{2}(p+1)A_j^2(1-\alpha_j)^2\alpha_j^{2i}. \tag{6.27}$$

Since α_j is already specified by Eqn. 6.16, our only free variables are A_j and B_j, so we can express B_j in terms of A_j:

$$B_j = A_j^2 \frac{(p+1)(1-\alpha_j)^2\alpha_j^2}{2(\alpha_j^2 - p)(\alpha_j^2 - 1)} \tag{6.28}$$

Our third term on the right hand side, $A_1 A_2 \alpha_1^i \alpha_2^i (1-\alpha_1)(1-\alpha_2)$, is a bit more complicated. If we plug in our expressions for α_1 and α_2 and simplify, we find that $(1-\alpha_1)(1-\alpha_2)$ becomes $-r$. Furthermore, $\alpha_1\alpha_2 = p$, so we can rewrite our right hand side as

$$(p+1)A_1A_2\alpha_1^i\alpha_2^i(1-\alpha_1)(1-\alpha_2) = -(p+1)A_1A_2rp^i. \tag{6.29}$$

Naievely, we want to guess a solution for $\tilde{b}_i$ of the form $B_3 p^i$; however, note from Eqn. 6.25 that terms of this form satisfy the homogeneous equation and therefore will give us 0 on the left hand side. This suggests then that we should try a different ansatz for this case; let us suppose, in analogy to the typical assumption for differential equations when we encounter a situation like this, that

$$\tilde{b}_i = B_3 i p^i. \tag{6.30}$$

We might worry that this solution will not vanish as $i \to -\infty$, but since the exponential

will shrink faster than the factor of i will approach $-\infty$, this condition is still satisfied. We can now plug in this ansatz, which gives us

$$B_3(i+1)p^{i+1} - B_3(p+1)ip^i + B_3p(i-1)p^{i-1} = -(p+1)A_1A_2rp^i. \tag{6.31}$$

Dividing through by p^{i-1}, we can write this as

$$B_3(i-1)\left[p^2-(p+1)p+p\right] + B_3\left[2p^2-(p+1)p\right] = -(p+1)A_1A_2rp. \tag{6.32}$$

The first term in brackets will go to 0, and thus we can conclude

$$B_3 = A_1A_2\frac{(p+1)r}{1-p} \tag{6.33}$$

Therefore, adding our three non-homogeneous solutions, as well as our homogeneous p^i solution, we find that in general,

$$\begin{aligned}\tilde{b}_i = Cp^i &+ A_1^2\frac{(p+1)(1-\alpha_1)^2\alpha_1^2}{2(\alpha_1^2-p)(\alpha_1^2-1)}\alpha_1^{2i} + A_2^2\frac{(p+1)(1-\alpha_2)^2\alpha_2^2}{2(\alpha_2^2-p)(\alpha_2^2-1)}\alpha_2^{2i} \\ &+ A_1A_2\frac{(p+1)r}{1-p}ip^i.\end{aligned} \tag{6.34}$$

Substituting in for α_1 and α_2, this becomes explicitly

$$\begin{aligned}\tilde{b}_i = Cp^i &+ A_1^2\frac{(p+1)(1\mp p^{\Delta_\phi})^2p^{2\Delta_\phi}}{2(p^{2\Delta_\phi}-p)(p^{2\Delta_\phi}-1)}p^{2\Delta_\phi i} \\ &+ A_2^2\frac{(p+1)(1\mp p^{-\Delta_\phi+1})^2p^{-2\Delta_\phi+2}}{2(p^{-2\Delta_\phi+2}-p)(p^{-2\Delta_\phi+2}-1)}p^{2(-\Delta_\phi+1)i} + A_1A_2\frac{(p+1)r}{1-p}ip^i,\end{aligned} \tag{6.35}$$

where we take the minus signs if $r = -1-p+\left(p^{\Delta_\phi}+p^{-\Delta_\phi+1}\right)$ and the plus signs if $r = -1-p-\left(p^{\Delta_\phi}+p^{-\Delta_\phi+1}\right)$. Note that in a number of cases, this equation will simplify because either A_1 or A_2 will be 0.

This entire discussion relied on the assumption that ϕ_i was a small number that we could represent as $\lambda\tilde{\phi}_i$. However, Eqn. 6.17 says that at arbitrarily large values of i, $\tilde{\phi}$ will be arbitrarily big. Therefore, we note that this solution only works down to some specific level in the tree, at which point it must break down as perturbation theory will no longer apply.

We can get a general sense for how ϕ and b behave as we move down in the tree by plotting them as a function of depth (i), picking some arbitrary values for our constants;we

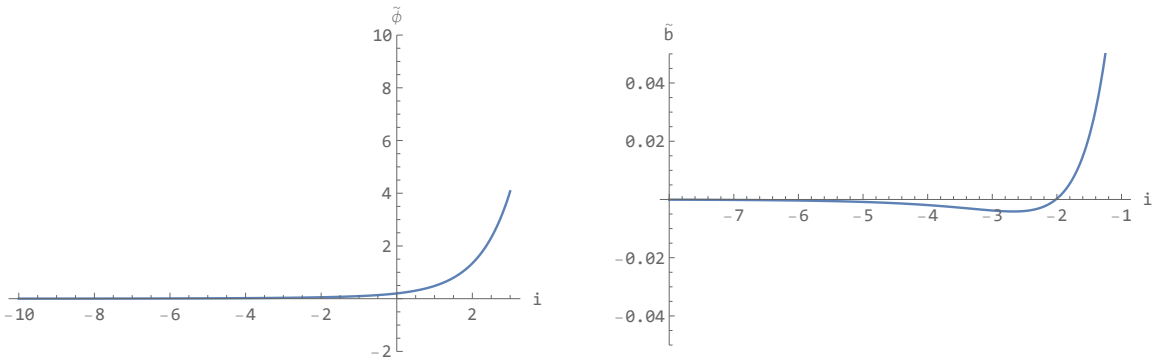

Figure 6.2: *Graphs of the of the scaling of $\tilde{\phi}_i$ and $\tilde{b}_i$ as a function of i. We see that both starts to grow exponentially on the right, as we expect from our equations; at some i, our solutions will blow up. To the left however, both are well-behaved. Here, $p = 5$, $\Delta_\phi = 0.75$, $r = -p - 1 + p^{0.75} + p^{0.25}$, and $A_1 = A_2 = C = 0.1$.*

have plotted $\tilde{\phi}$ and $\tilde{b}$ with representative constants in Fig. 6.2. Note that we have intentionally picked a value for Δ_ϕ such that we can make both A_1 and A_2 non-zero; if we set one of these to 0, we would not have the small bump we see in the $\tilde{b}$ graph of Fig. 6.2.

6.2 Radially Symmetric Solutions

In the previous section, we assumed that the length of an edge depended only on its depth in the tree, which we could also consider to be its distance from the boundary. In this section, however, we would like to consider a solution in which the value of a vertex or the length of an edge depends only on its distance from some arbitrary point in the bulk, which we will label as s. A visual representation of this is given in Fig. 6.3.

At an arbitrary distance, i steps away from s (where the closest vertices to s are at distance $i = 1$ and the edges connected to s are also at $i = 1$), any given vertex will have p neighbors that are 1 step further away from s and will have one neighbor that is one step closer to s. As an example, note that in Fig. 6.3, if we sum over all neighbors of an orange vertex (at $i = 2$), we will find it has $p = 3$ blue neighbors at $i = 3$, connected by an edge at $i = 3$, and one red neighbor at $i = 1$, connected by an edge at $i = 2$. Therefore, we can rewrite the sum in Eqn. 5.15 as

$$p b_{i+1}^2 \left(\phi_i - \phi_{i+1}\right) + b_i^2 \left(\phi_i - \phi_{i-1}\right) = -\frac{\partial V(\phi_i)}{\partial \phi_i} \tag{6.36}$$

Similarly, any given edge will have p neighbors that are a step further away from s, plus itself, all meeting at its further vertex, and it will have p neighbors at the same distance

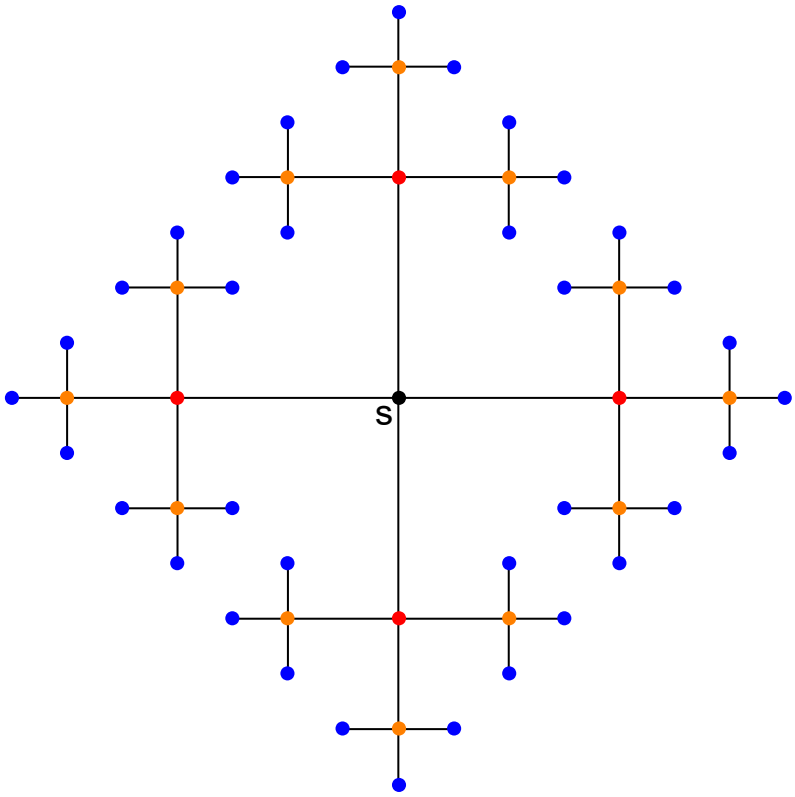

Figure 6.3: *We have redrawn this $p = 3$ tree to reflect the symmetry of the values the various edges and vertices take. Our central point is black and labeled s. Vertices of a given color all have the same value, becuase they are all the same distance from s; similarly, edges that have the same color vertices as their endpoints are also the same length as each other. For example, all edges that connect blue and orange points are the same length. In particular, we note that the red vertices are at distance $i = 1$, the orange vertices are at $i = 2$, the blue at $i = 3$, etc. Similarly, the edges connecting the black vertex to the red vertices are at distance $i = 1$, edges connecting red and orange vertices are at $i = 2$, those connecting orange and blue vertices are at $i = 3$, etc. Note that edge lengths are drawn for aesthetic convenience, not with correct lengths relative to each other.*

from s (including itself), plus one edge that is a step closer, meeting at its closer vertex. As an example, consider an edge between a red and an orange vertex: at the orange vertex, the sum over all edges that include that vertex will be $pb_3 + b_2$, and at the red vertex, the sum of all edges that include that vertex will be $pb_2 + b_1$. Therefore, we can expand the sums in Eqn. 5.14 to obtain the Einstein equation

$$\begin{aligned} b_i \frac{(pb_i + b_{i-1})^2}{\left(pb_i^2 + b_{i-1}^2\right)^2} - \frac{pb_i + b_{i-1}}{pb_i^2 + b_{i-1}^2} \\ + b_i \frac{(pb_{i+1} + b_i)^2}{\left(pb_{i+1}^2 + b_i^2\right)^2} - \frac{pb_{i+1} + b_i}{pb_{i+1}^2 + b_i^2} = -\frac{1}{2}\left(\phi_i - \phi_{i-1}\right)^2, \end{aligned} \tag{6.37}$$

which we can rearrange to get

$$\begin{aligned}&\left((1-p)b_ib_{i-1}^2+pb_i^2b_{i-1}-b_{i-1}^3\right)\left(pb_{i+1}^2+b_i^2\right)^2\\&+\left((p^2-p)b_{i+1}^2b_i+pb_i^2b_{i+1}-p^2b_{i+1}^3\right)\left(pb_i^2+b_{i-1}^2\right)^2\\&\qquad=-\frac{1}{2}\left(\phi_i-\phi_{i-1}\right)^2\left(pb_i^2+b_{i-1}^2\right)^2\left(pb_{i+1}^2+b_i^2\right)^2.\end{aligned}\tag{6.38}$$

However, at s things become slightly more complicated, as the values of neighbors do not follow the same pattern as they do far from s. In particular, when $i=0$, namely when we are looking at the vertex s, s will have $p+1$ neighbors all with the same value as each other (all will be red dots). Therefore, in this case Eqn. 5.15 becomes

$$(p+1)b_1^2(\phi_0-\phi_1)=-\frac{\partial V(\phi_0)}{\partial\phi_0}.\tag{6.39}$$

For similar reasons, when $i=1$, our Einstein equation will change. From Eqn. 5.14, we see that if we assume that x labels the vertex s and y labels one of its neighbors, the third and fourth terms on the left hand side will take the same form as the third and fourth terms on the left hand side of Eqn. 6.37. The first and second terms, however, will instead have the following form:

$$b_1\frac{((p+1)b_1)^2}{((p+1)b_1^2)^2}-\frac{(p+1)b_1}{(p+1)b_1^2}=\frac{b_1^3}{b_1^4}-\frac{b_1}{b_1^2}=0.\tag{6.40}$$

Therefore, at $i=1$, our Einstein equation becomes

$$b_1\frac{(pb_2+b_1)^2}{(pb_2^2+b_1^2)^2}-\frac{pb_2+b_1}{pb_2^2+b_1^2}=-\frac{1}{2}(\phi_0-\phi_1)^2\tag{6.41}$$

which simplifies to

$$(p^2-p)b_2^2b_1+pb_2b_1^2-p^2b_2^3=-\frac{1}{2}\left(\phi_0-\phi_1\right)^2\left(pb_2^2+b_1^2\right)^2\tag{6.42}$$

As before, we assume that ϕ_x will be very small and b_{xy} will only deviate slightly from 1, making a ansätze of the form of Eqns. 6.4 and 6.5 and expecting that as $i\to\infty$, ϕ_i will vanish and $b_i\to 1$. In this geometry, we may in fact be able to satisfy our ansätze for the entirety of the tree. In the previous section, we ran into the problem that if ϕ_i vanished as $i\to-\infty$, it would blow up as $i\to\infty$. In this geometry, however, i is never less than 0, and we will therefore not encounter a similar problem. Taking these ansätze and expanding our Einstein equation to order λ^2 and our Klein-Gordon equation to order λ, and also making the substitution as we did in the previous section that $\left.\frac{\partial^2V(\phi_i)}{\partial\phi_i^2}\right|_{\phi_i=0}=r$, we find that Eqn.

6.36 becomes

$$p\tilde{\phi}_{i+1} - (p+1+r)\tilde{\phi}_i + \tilde{\phi}_{i-1} = 0, \tag{6.43}$$

for $i \geq 1$, while the Klein-Gordon equation for the point s (Eq. 6.39) becomes

$$(p+1)\left(\tilde{\phi}_0 - \tilde{\phi}_1\right) = -r\tilde{\phi}_0. \tag{6.44}$$

Furthermore, Eqn. 6.38 will become

$$p\tilde{b}_{i+1} - (p+1)\tilde{b}_i + \tilde{b}_{i-1} = \frac{1}{2}(\tilde{\phi}_i - \tilde{\phi}_{i-1})^2(p+1) \tag{6.45}$$

for $i \geq 2$, and similarly the equation for $i = 1$ (Eqn. 6.42) will become

$$-p\tilde{b}_2 + p\tilde{b}_1 = -\frac{1}{2}(\tilde{\phi}_0 - \tilde{\phi}_1)^2(p+1). \tag{6.46}$$

We will consider Eqns. 6.44 and 6.46 as boundary conditions for solutions to the general equations, Eqns. 6.43 and 6.45 respectively.

We now turn to finding general solutions of Eqn. 6.43, which we solve first because it appears at first glance less complicated than Eqn. 6.45. As is typical for solving homogeneous difference equations, we make the same ansatz as in Eqn. 6.11, that our solution is proportional to some number α raised to the power of i, its distance from s. Plugging in and solving, we find, in a similar fashion to Eqn. 6.16,

$$\alpha_{1,2} = \frac{(p+1+r) \pm \sqrt{(p+1+r)^2 - 4p}}{2p}, \tag{6.47}$$

which, if we again parametrize r by setting it equal to $-1-p\pm\left(p^{\Delta_\phi} + p^{-\Delta_\phi+1}\right)$, simplifies our solutions to

$$\alpha_1 = \pm p^{\Delta_\phi - 1}; \qquad \alpha_2 = \pm p^{-\Delta_\phi}, \tag{6.48}$$

where again, either both solutions are positive or both are negative.

Therefore, our solution in general is

$$\tilde{\phi}_i = A_1(\pm 1)^i p^{(\Delta_\phi - 1)i} + A_2(\pm 1)^i p^{-\Delta_\phi i}. \tag{6.49}$$

We now take this general solution and impose the boundary condition by plugging it in

to Eqn. 6.44. From this, we get

$$\begin{aligned}(p+1)\left[A_1+A_2\mp\left(A_1p^{(\Delta_\phi-1)}+A_2p^{-\Delta_\phi}\right)\right] &= -r(A_1+A_2)\\ &= -\left(-1-p\pm\left(p^{\Delta_\phi}+p^{-\Delta_\phi+1}\right)\right)(A_1+A_2)\end{aligned} \tag{6.50}$$

which can be rearranged to give

$$A_2 = A_1\frac{p^{\Delta_\phi-1}-p^{-\Delta_\phi+1}}{p^{\Delta_\phi}-p^{-\Delta_\phi}} = A_1\frac{p^2-p^{2\Delta_\phi}}{p-p^{2\Delta_\phi+1}}. \tag{6.51}$$

Consequently, we conclude

$$\tilde{\phi}_i = A_1(\pm1)^i p^{(\Delta_\phi-1)i} + A_1(\pm1)^i\frac{p^2-p^{2\Delta_\phi}}{p-p^{2\Delta_\phi+1}}p^{-\Delta_\phi i} \tag{6.52}$$

which we can write more conveniently as

$$\tilde{\phi}_i = A_1\alpha_1^i + A_2\alpha_2^i \tag{6.53}$$

where A_2 is given in Eqn. 6.51 and α_1 and α_2 are given in Eqn. 6.48.

As before, we want the solution for ϕ_i to vanish on the boundary, and in this convention this means that as $i\to\infty$ (since each increase in i is a step outward toward the boundary), we want $\phi_i\to 0$. However, Eqn. 6.51 tells us that A_1 is directly proportional to A_2, so therefore we cannot set one to 0 without setting both to 0. Therefore, in order for the ϕ field to vanish when $i\to\infty$, we require that both α_1 and α_2 simultaneously have absolute value less than 1. From Eqn. 6.48, this in turn means that we require

$$0<\Delta_\phi<1. \tag{6.54}$$

Having found a solution for $\tilde{\phi}_i$, namely Eqn. 6.52, we now turn to our other equation of motion, Eqn. 6.45. First, we must solve the homogeneous equation, where the left hand side is equal to 0. To do this, we posit a solution of the form

$$\tilde{b}_i = C\omega^i \tag{6.55}$$

Then we must simply solve the equation

$$p\omega^2-(p+1)\omega+1=0, \tag{6.56}$$

which leads us to the solutions

$$\omega = \frac{1}{p}; \qquad \omega = 1. \tag{6.57}$$

Since we saw that our solutions to the ϕ equation were proportional to $p^{\Delta_\phi - 1}$ and $p^{-\Delta_\phi}$, we hope this should be the case for the graviton too, but with Δ_ϕ replaced by Δ_J. If we set Δ_J equal to 1 or 0, so that we get a massless graviton in Eqn. 4.15, this indeed gives us solutions proportional to p^{-1} and p^0, matching Eqn. 6.57. As before, we ignore the second of these solutions as it does not fall off to 0 when taken to a large power.

The inhomogeneous situation is more complicated, but our approach mimics the method we used in the previous section. The right hand side of Eqn. 6.45 can be expanded, after plugging in Eqn. 6.53, as

$$\begin{aligned}\frac{1}{2}(\tilde{\phi}_i - \tilde{\phi}_{i-1})^2(p+1) &= \frac{1}{2}(p+1)\left(A_1\alpha_1^i + A_2\alpha_2^i - A_1\alpha_1^{i-1} - A_2\alpha_2^{i-1}\right)^2 \\ &= \frac{1}{2}(p+1)\big[A_1^2\alpha_1^{2i-2}(\alpha_1-1)^2 + A_2^2\alpha_2^{2i-2}(\alpha_2-1)^2 \\ &\qquad + 2A_1A_2\alpha_1^{i-1}\alpha_2^{i-1}(\alpha_1-1)(\alpha_2-1)\big].\end{aligned} \tag{6.58}$$

In the same vein as before, we will solve the inhomogeneous equation by separately taking each of the three additive terms in the last two lines of Eqn. 6.58 as the right hand side of our inhomogeneous equation, and our total inhomogeneous solution will be the sum of these three individual inhomogeneous solutions. For the terms on the second line of Eqn. 6.58, we take the RHS to be

$$\frac{1}{2}(p+1)A_j^2\alpha_j^{2i-2}(\alpha_j-1)^2,$$

where j can be either 1 or 2, and for each j we posit an ansatz of the form given in Eqn. 6.26. Thus, our equation becomes

$$pB_j\alpha_j^{2i+2} - (p+1)B_j\alpha_j^{2i} + B_j\alpha_j^{2i-2} = \frac{1}{2}(p+1)A_j^2\alpha_j^{2i-2}(\alpha_j-1)^2. \tag{6.59}$$

Dividing through by α_j^{2i-2} and solving for B_j, we find

$$B_j = A_j^2\frac{(p+1)(\alpha_j-1)^2}{2(p\alpha_j^2-1)(\alpha_j^2-1)}. \tag{6.60}$$

For the term on the last line of from Eqn. 6.58, we notice that given α_1 and α_2 as in Eqn. 6.48, the product of $(1-\alpha_1)(1-\alpha_2)$ is $-\frac{r}{p}$ and the product of $\alpha_1\alpha_2$ is $\frac{1}{p}$. This means

our inhomogeneous term on the left hand side will be proportional to $\frac{1}{p^i}$. Our intial guess for a solution to this equation might be a term also proportional to $\frac{1}{p^i}$; however, we found in Eqn. 6.57 that terms like this are solutions to the homogeneous equation and therefore will always give us 0 on the left hand side. Therefore, we instead assume an ansatz of the form

$$\tilde{b}_i = B_3 i \frac{1}{p^i} \tag{6.61}$$

Plugging this in, we find[

$$pB_3(i+1)\frac{1}{p^{i+1}} - (p+1)B_3 i\frac{1}{p^i} + B_3(i-1)\frac{1}{p^{i-1}} = -A_1A_2(p+1)\frac{r}{p}\frac{1}{p^i}. \tag{6.62}$$

Here, we can multiply by p^{i+1}, and we can separate out the left hand side into $B_3(i-1)\left[p-(p+1)p+p^2\right]+B_3\left[2p-(p+1)p\right]$, where the expression inside the first set of brackets will vanish. Therefore, we conclude

$$B_3 = A_1A_2\frac{(p+1)r}{p-1} \tag{6.63}$$

Now we can add up the three inhomogeneous solutions, plus the homogeneous solution of interest, to find

$$\begin{aligned}\tilde{b}_i = C\frac{1}{p^i} &+ A_1^2\frac{(p+1)(\alpha_1-1)^2}{2(p\alpha_1^2-1)(\alpha_1^2-1)}\alpha_1^{2i} + A_2^2\frac{(p+1)(\alpha_2-1)^2}{2(p\alpha_2^2-1)(\alpha_2^2-1)}\alpha_2^{2i} \\ &+ A_1A_2\frac{(p+1)r}{p-1}i\frac{1}{p^i},\end{aligned} \tag{6.64}$$

which we can write more explicitly as

$$\begin{aligned}\tilde{b}_i = C\frac{1}{p^i} &+ A_1^2\frac{(p+1)(1\mp p^{\Delta_\phi-1})^2}{2(p^{2\Delta_\phi-1}-1)(p^{2\Delta_\phi-2}-1)}p^{2(\Delta_\phi-1)i} \\ &+ A_1^2\left(\frac{p^2-p^{2\Delta_\phi}}{p-p^{2\Delta_\phi+1}}\right)^2\frac{(p+1)(1\mp p^{-\Delta_\phi})^2}{2(p^{-2\Delta_\phi+1}-1)(p^{-2\Delta_\phi}-1)}p^{-2\Delta_\phi i} \\ &+ A_1^2\left(\frac{p^2-p^{2\Delta_\phi}}{p-p^{2\Delta_\phi+1}}\right)\frac{(p+1)r}{p-1}i\frac{1}{p^i},\end{aligned} \tag{6.65}$$

or more compactly,

$$\tilde{b}_i = C\frac{1}{p^i} + B_1\alpha_1^{2i} + B_2\alpha_2^{2i} + B_3 i\frac{1}{p^i}, \tag{6.66}$$

where B_1 and B_2 are as expressed in Eqn. 6.60 and B_3 is as expressed in Eqn. 6.63 and α_1 and α_2 are as expressed in Eqn. 6.48.

Now all that remains is to impose the boundary condition given by Eqn. 6.46. Plugging

in our solution from Eqn. 6.66, and noting from Eqn. 6.44 that $(\tilde{\phi}_0 - \tilde{\phi}_1)(p+1) = -r\tilde{\phi}_0$ we find

$$\begin{aligned}\frac{-(r(A_1+A_2))^2}{2(p+1)} &= p\left[C\frac{1}{p} + B_1 p^{2\Delta_\phi - 2} + B_2 p^{-2\Delta_\phi} + B_3\frac{1}{p}\right] \\ &\quad -p\left[C\frac{1}{p^2} + B_1 p^{4\Delta_\phi - 4} + B_2 p^{-4\Delta_\phi} + B_3\frac{2}{p^2}\right],\end{aligned} \tag{6.67}$$

$$\begin{aligned}\Rightarrow C = \frac{p^2}{p-1}\Bigg[&\frac{-(rA_1 + rA_2)^2}{2p(p+1)} + B_1(p^{4\Delta_\phi - 4} - p^{2\Delta_\phi - 2}) \\ &+ B_2(p^{-4\Delta_\phi} - p^{-2\Delta_\phi}) + B_3\left(\frac{2-p}{p^2}\right)\Bigg]\end{aligned} \tag{6.68}$$

Therefore, we have completely specified a perturbative solution to this radially symmetric geometry. In summary, we will have some Δ_ϕ, given by the value of r in our action, but that can only lie in the range given by Inequality 6.54. Given this Δ_ϕ, we solve for our α_1 and α_2 as given by Eqn. 6.48. We are free to scale our solution arbitrarily by our choice of A_1, but we find that to satisfy conditions at the central point s, A_2 must be given by Eqn. 6.51 such that our solution for $\tilde{\phi}_i$ is as given by Eqn. 6.52. Furthermore, we can solve for the edge length fluctuations $\tilde{b}_i$ as in Eqn. 6.66, where the constants B_1 and B_2 are as given in Eqn. 6.60 for appropriate values of j, B_3 is as given by Eqn. 6.63, and C is as given by Eqn. 6.68.

Thus, we have shown that though the solutions are more limited than in the case where values depend on the depth in the tree, we can find consistent solutions in which the fields b and ϕ take radially symmetric solutions around some point s. We can also track schematically how $\tilde{\phi}_i$ and $\tilde{b}_i$ evolve with i by plotting them as a function of i; Fig. 6.4 plots their values as a function of i with representative constants.

The fact that we get a more limited solution here makes sense, because we have imposed more constraints on the system than we did in the previous section. before imposing any boundary conditions, we have four "free" parameters: A_1, A_2, C, and Δ_ϕ (the parameters B_1, B_2, and B_3 aren't really free parameters, as they are the coefficients for the inhomogeneous solution). In Section 6.1, only one of these needed to be fixed in order to satisfy our single boundary condition, that the ϕ field vanishes at the edge of the tree. To accomplish this, we could either fix Δ_ϕ to be in the range given by Inequality 6.20, or we could fix one of our A's to be 0 (depending on the value of Δ_ϕ). In this section, we imposed two more constraints, in the form of Eqns. 6.44 and 6.46, describing what should happen at the central point s. Therefore, we expect two more of our constants to be fixed to satisfy

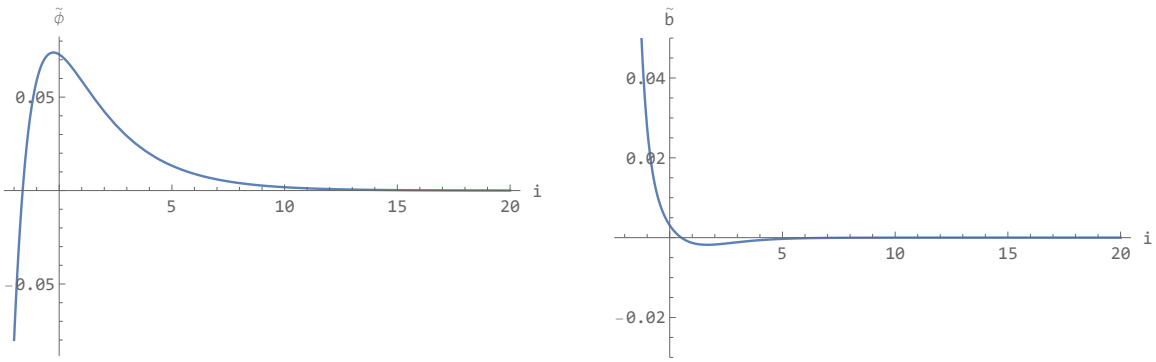

Figure 6.4: *Graphs for the of the scaling of $\tilde{\phi}_i$ and $\tilde{b}_i$ as a function of i, in the case when the value depends on the distance from a central point s. We are only concerned with i values greater than 0, and in this regime we see that both $\tilde{\phi}$ and $\tilde{b}$ remain bounded, which is exactly what we want. Here, $p = 5$, $\Delta_\phi = 0.75$, $R = -p - 1 + p^{0.75} + p^{0.25}$, and $A_1 = 0.1$.*

these conditions, and indeed, we find that in our solution here, Δ_ϕ is fixed to satisfy the condition at $i = \infty$, A_2 is fixed to satisfy the boundary condition in Eqn. 6.44, and C is fixed to satisfy the boundary condition in Eqn. 6.46, leaving only A_1 as a free parameter.

6.3 Altering the Geometry: A Radial Solution on the Almost-Tree

Until now, we have only considered the Bruhat-Tits tree as is, with no modifications regarding its structure. However, we can introduce the concept of loops into the tree. Physically, a loop in a tree corresponds to a Euclidean black hole in the AdS space, meaning it is a black hole that has been Wick-rotated from Minkowski space [13]. Gubser et al. note in their paper that their derivation of the "curvature" on the Bruhat-Tits tree, (κ_{xy}, as defined in Equation 19 in their paper or by Eqn. 5.4 in this thesis) holds on a tree with cycles, but only if the cycles have at least 7 edges and each edge length is within a factor of $\frac{4}{3}$ of all other edge lengths in the loop [1]. With these qualifications in mind, we can consider a lattice with one such loop, where for our purposes the number of nodes in this loop is irrelevant, so long as it is more than 7. On this loop, every vertex will have $p - 1$ copies of the Bruhat-Tits tree attached to it emerging outward from the ring, so that these nodes, like every other node in the tree, have coordination number $p + 1$. Figure 6.5 shows this structure for $p = 3$, with 8 nodes in the central ring. We will call this geometry with one ring an "almost-tree."

We now set out to solve our equations of motion on this almost-tree. With this tree geometry, the most natural geometry for the fields is for them to assume radial symmetry

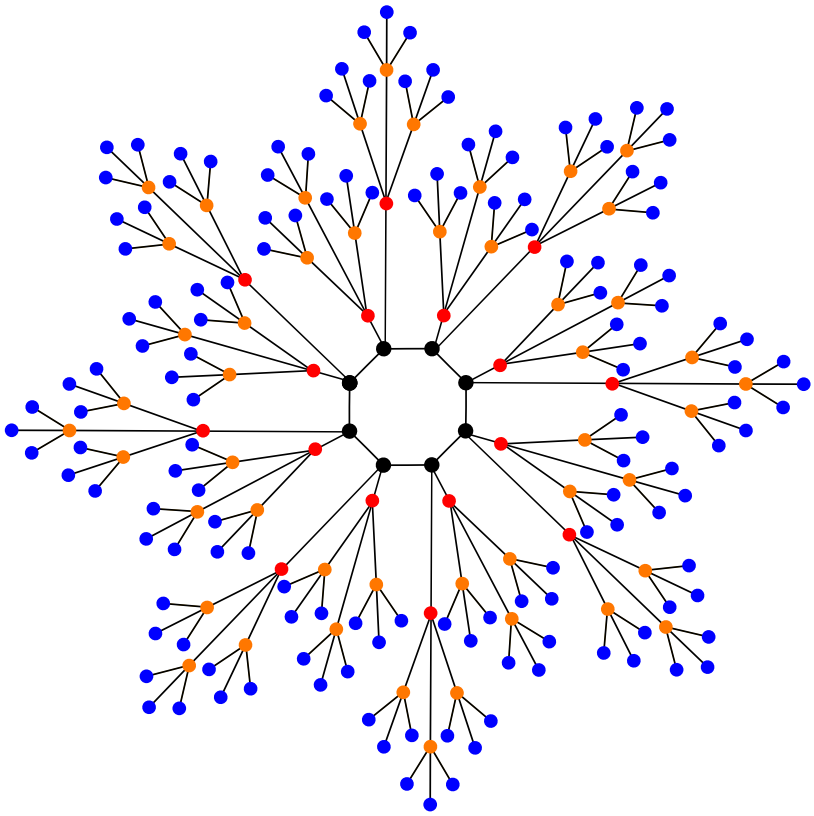

Figure 6.5: *Depicted here is a $p = 3$ almost-tree, in which we have put the loop in the center of the figure to highlight the symmetry. Vertices of a given color all have the same values as each other because they are all the same distance from the ring: the black vertices are at distance $i = 0$, the red vertices are at $i = 1$, the orange at $i = 2$, and the blue at $i = 3$. Similarly, all edges with the same color end points as each other will be the same length; this means that all edges that end in one black and one red vertex are at distance $i = 1$, those that connect red and orange vertices are at $i = 2$, and those that connect orange and blue vertices are $i = 3$. Edges that connect two black vertices on the ring are considered separately. Note that edge lengths are drawn for aesthetic convenience, not with correct lengths relative to each other.*

around the loop, such that the number of steps from the ring determines the value of a vertex or edge. Consequently, this means all edge lengths and vertex values on the ring itself must be the same as each other, as they are all distance 0 from the ring.

We start, therefore, by considering an edge b_{xy} that is part of the ring. This means that ϕ_x and ϕ_y must take the same value as each other, so the right hand side of Eqn. 5.14 is 0. Furthermore, since x has 2 neighbors on the ring and $p - 1$ neighbors at $i = 1$ (sprouting from the ring), and y has the same arrangement of neighbors, the first and third terms of the left hand side will be identical to each other, as will the second and fourth. Therefore, if we call the b value associated with an edge in the ring A and we call the b value of an

edge sprouting from the ring B, Eqn. 5.14 becomes

$$2\left(A\frac{((p-1)B+2A)^2}{((p-1)B^2+2A^2)^2}-\frac{(p-1)B+2A}{(p-1)B^2+2A^2}\right)=0. \tag{6.69}$$

Multiplying through by a common denominator and simplifying, we find this simplifies to

$$0=(p-3)(p-1)AB^2+2(p-1)A^2B-(p-1)^2B^3=-(p-1)B((p-1)B+2A)(B-A) \tag{6.70}$$

Thus, we see our solutions are

$$B=A; \qquad B=-\frac{2}{p-1}A; \qquad B=0 \tag{6.71}$$

where for our purposes only the first solution makes physical sense as an inverse length. Therefore, we see that the edges of the ring must be the same length as the edges coming out of the ring.

We now consider an edge b_{xy} that sprouts from the ring (it will be at level $i=1$). Because $b_{xy}=b_{xx_i}\forall i$, assuming x is the vertex on the ring, we therefore only have to consider the third and fourth terms in Eqn. 5.14. To see this, note that if the b value of the shoots emanating from the ring, B, is equal to the b value of the edges on the ring, A, then first two terms will reduce to

$$B\frac{((p-1)B+2A)^2}{((p-1)B^2+A^2)^2}-\frac{(p-1)B+2A}{(p-1)B^2+2A^2}\Rightarrow\frac{(p+1)^2A^3}{(p+1)^2A^4}-\frac{(p+1)A}{(p+1)A^2}=0 \tag{6.72}$$

We also now begin labeling vertices and edges explicitly by their distance from the ring, such that b_1 is the first shoot emanating from the ring, b_2 is a step further out, etc., and ϕ_0 is a vertex on the ring, ϕ_1 is a neighbor to the ring, etc. Therefore when considering $\langle xy\rangle$ to be an edge sprouting from the ring, our Einstein equation 5.14 becomes

$$b_1\frac{(pb_2+b_1)^2}{(pb_2^2+b_1^2)^2}-\frac{pb_2+b_1}{pb_2^2+b_1^2}=-\frac{1}{2}(\phi_0-\phi_1)^2, \tag{6.73}$$

which can be simplified to

$$(p^2-p)b_2^2b_1+pb_2b_1^2-p^2b_2^3=-\frac{1}{2}\left(\phi_0-\phi_1\right)^2(pb_2^2+b_1^2)^2. \tag{6.74}$$

Further out from the ring, our geometry is the same as in the previous section, because for any given edge, it will have p neighbors a step further out, $p-1$ neighbors at the same

distance, and one neighbor a step closer in. Therefore, our Einstein equation for $i \geq 2$ is the same as Eqn. 6.38:

$$\begin{aligned}&\left((1-p)b_i b_{i-1}^2 + pb_i^2 b_{i-1} - b_{i-1}^3\right)\left(pb_{i+1}^2 + b_i^2\right)^2 \\ &+ \left((p^2-p)b_{i+1}^2 b_i + pb_i^2 b_{i+1} - p^2 b_{i+1}^3\right)\left(pb_i^2 + b_{i-1}^2\right)^2 \\ &\qquad = -\frac{1}{2}\left(\phi_i - \phi_{i-1}\right)^2\left(pb_i^2 + b_{i-1}^2\right)^2\left(pb_{i+1}^2 + b_i^2\right)^2\end{aligned} \tag{6.75}$$

For the same reasons, our Klein-Gordon equation of motion will be identical to Eqn. 6.36 from the previous section:

$$pb_{i+1}^2\left(\phi_i - \phi_{i+1}\right) + b_i^2\left(\phi_i - \phi_{i-1}\right) = -\frac{\partial V(\phi_i)}{\partial \phi_i} \tag{6.76}$$

which will hold for $i \geq 1$. This makes sense, as the only difference between the radially symmetric tree and the radially symmetric almost-tree is what happens at their centers. In particular, with this almost-tree geometry, if we consider a vertex x on the ring, we see that it will have two neighbors also on the ring, which will have the same value as x, and therefore they will contribute 0 when we take the sum of $\phi_x - \phi_y$ for all neighbors y of x. The only contribution to our sum, therefore, will be from the $p-1$ vertices at $i = 1$; this means our Klein-Gordon equation of motion for vertices on the ring (which we label as ϕ_0) is

$$(p-1)b_1^2\left(\phi_0 - \phi_1\right) = -\frac{\partial V(\phi_0)}{\partial \phi_0}. \tag{6.77}$$

As before, wish to solve these equations perturbatively. To do so, we assume ansätze for ϕ and b as given by Eqns. 6.4 and 6.5, and we further assume, as we have previously, that $\left.\frac{\partial^2 V(\phi_i)}{\partial \phi_i^2}\right|_{\phi_i=0} = r$. This transforms our general equations, Eqns. 6.76 and 6.75, into

$$p\tilde{\phi}_{i+1} - (p+1+r)\tilde{\phi}_i + \tilde{\phi}_{i-1} = 0. \tag{6.78}$$

and

$$p\tilde{b}_{i+1} - (p+1)\tilde{b}_i + \tilde{b}_{i-1} = \frac{1}{2}(\tilde{\phi}_i - \tilde{\phi}_{i-1})^2(p+1) \tag{6.79}$$

respectively, and it transforms the equations for near the ring, Eqns. 6.77 and 6.74, into

$$(p-1)\tilde{\phi}_1 - (p-1+r)\tilde{\phi}_0 = 0. \tag{6.80}$$

and

$$-p\tilde{b}_2 + p\tilde{b}_1 = -\frac{1}{2}(\tilde{\phi}_0 - \tilde{\phi}_1)^2(p+1). \tag{6.81}$$

respectively. As before, we will take Eqns. 6.80 and 6.81 as imposing boundary conditions on the general solutions of Eqns. 6.78 and 6.79 respectively.

As in the previous sections, we begin first by solving the equations involving only ϕ, as they are easier to solve. Because Eqn. 6.78 is the same as Eqn. 6.43, its solutions will also be the same, namely

$$\tilde{\phi}_i = A_1(\pm 1)^i p^{(\Delta_\phi - 1)i} + A_2(\pm 1)^i p^{-\Delta_\phi i}. \tag{6.82}$$

and in particular, we find again that our solutions for α are

$$\alpha_1 = \pm p^{\Delta_\phi - 1}; \qquad \alpha_2 = \pm p^{-\Delta_\phi}, \tag{6.83}$$

where Δ_ϕ is specified by r through the relationship $r = -1 - p \pm \left(p^{\Delta_\phi} + p^{-\Delta_\phi + 1}\right)$, and in Eqn. 6.83, either both α's are positive or both are negative.

Now we must simply impose the constraints of Eqn. 6.80, which requires that

$$(p-1)\left(A_1 + A_2 - A_1\alpha_1 - A_2\alpha_2\right) = -r(A_1 + A_2) \tag{6.84}$$

which simplifies to

$$A_2 = A_1 \frac{2 \mp \left(p^{\Delta_\phi - 1} + p^{-\Delta_\phi + 1}\right)}{-2 \pm \left(p^{\Delta_\phi} + p^{-\Delta_\phi}\right)}. \tag{6.85}$$

Therefore,

$$\tilde{\phi}_i = A_1(\pm 1)^i p^{(\Delta_\phi - 1)i} + A_1(\pm 1)^i \frac{2 \mp \left(p^{\Delta_\phi - 1} + p^{-\Delta_\phi + 1}\right)}{-2 \pm \left(p^{\Delta_\phi} + p^{-\Delta_\phi}\right)} p^{-\Delta_\phi i}, \tag{6.86}$$

or expressed more compactly,

$$\tilde{\phi}_i = A_1\alpha_1^i + A_2\alpha_2^i \tag{6.87}$$

with α_1 and α_2 given in Eqn. 6.83 and A_2 given by Eqn. 6.85.

Since, as in the previous section, A_1 is directly proportional to A_2, we cannot set one arbitrarily to 0. Therefore, in order for the ϕ field to vanish infinitely at the boundary, we require that both α_1 and α_2 must have absolute value less than 1 so that the field strength of ϕ_i appraoches zero at large i. As before, then, we find from Eqn. 6.83 that Δ_ϕ must

satisfy

$$0 < \Delta_\phi < 1. \tag{6.88}$$

We also see that since our Einstein equation for any $i \geq 2$ (Eqn. 6.79) is the same as in the previous section (Eqn. 6.45), its general solution should be the same; that is, we find that the solution for the edge length fluctuations here is

$$\begin{aligned}\tilde{b}_i = C\frac{1}{p^i} + A_1^2\frac{(p+1)(\alpha_1-1)^2}{2(p\alpha_1^2-1)(\alpha_1^2-1)}\alpha_1^{2i} + A_2^2\frac{(p+1)(\alpha_2-1)^2}{2(p\alpha_2^2-1)(\alpha_2^2-1)}\alpha_2^{2i} \\ + A_1A_2\frac{(p+1)r}{p-1}i\frac{1}{p^i}.\end{aligned} \tag{6.89}$$

However, since this geometry produces a different relationship between A_1 and A_2, our A_2 value in Eqn. 6.89 will be as given in Eqn. 6.85. If we expand this more fully, we see explicitly:

$$\begin{aligned}\tilde{b}_i = C\frac{1}{p^i} + A_1^2\frac{(p+1)(1\mp p^{\Delta_\phi-1})^2}{2(p^{2\Delta_\phi-1}-1)(p^{2\Delta_\phi-2}-1)}p^{2(\Delta_\phi-1)i} \\ + A_1^2\left(\frac{2\mp\left(p^{\Delta_\phi-1}+p^{-\Delta_\phi+1}\right)}{-2\pm\left(p^{\Delta_\phi}+p^{-\Delta_\phi}\right)}\right)^2 p^{-2\Delta_\phi i} \\ + A_1^2\left(\frac{2\mp\left(p^{\Delta_\phi-1}+p^{-\Delta_\phi+1}\right)}{-2\pm\left(p^{\Delta_\phi}+p^{-\Delta_\phi}\right)}\right)\frac{(p+1)r}{p-1}i\frac{1}{p^i}.\end{aligned} \tag{6.90}$$

We can compactly notate this solution by writing

$$\tilde{b}_i = C\frac{1}{p^i} + B_1\alpha_1^{2i} + B_2\alpha_2^{2i} + B_3 i\frac{1}{p^i}, \tag{6.91}$$

using the defintions that

$$B_j = A_j^2\frac{(p+1)(\alpha_j-1)^2}{2(p\alpha_j^2-1)(\alpha_j^2-1)} \tag{6.92}$$

for $j = 1, 2$ and

$$B_3 = A_1A_2\frac{(p+1)r}{p-1}. \tag{6.93}$$

Finally, all that remains is for us to show that we can satisfy Eqn. 6.81 with this solution.

We see this leads us to

$$\begin{aligned}-\frac{1}{2}(\tilde{\phi}_0-\tilde{\phi}_1)^2(p+1) =& p\left[C\frac{1}{p}+B_1\alpha_1^2+B_2\alpha_2^2+B_3\frac{1}{p}\right]\\ &-p\left[C\frac{1}{p^2}+B_1\alpha_1^4+B_2\alpha_2^4+B_3\frac{2}{p^2}\right]\end{aligned} \tag{6.94}$$

Solving, and noting that $(p-1)\left(\tilde{\phi}_0-\tilde{\phi}_1\right)=-r(A_1+A_2)$ by Eqn. 6.80, we find that we must set

$$\begin{aligned}C=\frac{p^2}{p-1}\Bigg[&-(rA_1+rA_2)^2\frac{p+1}{2p(p-1)^2}\\ &+B_1\left(p^{4\Delta_\phi-4}-p^{2\Delta_\phi-2}\right)+B_2\left(p^{-4\Delta_\phi}-p^{-2\Delta_\phi}\right)+B_3\left(\frac{2-p}{p^2}\right)\Bigg]\end{aligned} \tag{6.95}$$

In the end, we find the solution for our equations when we assume our geometry is an almost-tree looks very similar to our solution for a radially symmetric field on a regular tree, with the primary difference being the different definition of A_2 (which in turn affects the definitions of B_2, B_3, and C). Our $\tilde{\phi}$ field is given by Eqn. 6.86, and our $\tilde{b}$ field is given by Eqn. 6.91, with constants B_1 and B_2 given by Eqn. 6.92, the constant B_3 given by Eqn. 6.93, the constant C given by Eqn. 6.95, and the values for α_1 and α_2 given by Eqn. 6.83. The similarity of this result to that found in the previous section is hardly surprising, as both represent effectively the same situation with different central boundary conditions. Since we impose two boundary conditions at the center, namely Eqns. 6.80 and 6.81, plus the boundary condition at the edge of the tree, we also expect, as in the previous section, that three of our "free" variables will be set by these boundary conditions; as before, Δ_ϕ is determined by the boundary condition at the boundary of the tree, A_2 is determined by Eqn. 6.80, and C is determined by 6.81, leaving only A_1 as a free parameter. We can see how our $\tilde{\phi}_i$ and $\tilde{b}_i$ scale as a function of i in Fig. 6.6, which plots these functions with representative constants chosen; we see, as we would hope, that they stay under control for all $i \geq 0$.

6.4 Operators in the CFT

In the Section 6.1, we found that if we wanted both A_1 and A_2 to be non-zero, we needed Δ_ϕ to be between 0 and 1; furthermore, in our solutions in Sections 6.2 and 6.3, we *required* that $0 < \Delta_\phi < 1$ in order for a solution to exist. Referring back to Eqn. 3.15, we see that this range of values for Δ_ϕ will make both ζ functions postitive, which in turn makes the

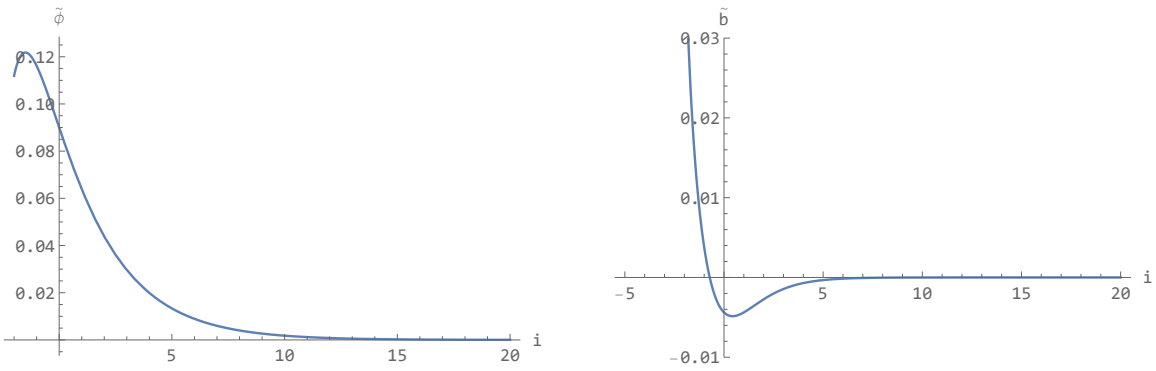

Figure 6.6: *These are graphs of the of the scaling of $\tilde{\phi}_i$ and $\tilde{b}_i$ as a function of i when assuming a radial geometry on the almost-tree. We are only concerned with the behavior for $i \geq 0$, and we see both graphs are well-behaved in this regime. Here, $p = 5$, $\Delta_\phi = 0.75$, $r = -p - 1 + p^{0.75} + p^{0.25}$, and $A_1 = 0.1$.*

mass term, $m_\phi^2 = r$, negative.

In order to expand upon further implications of this fact, we will delve slightly into the full AdS/CFT correspondance, and in particular we will bring in the conformal field theory side of the duality. By nature of being a conformal theory, the CFT is scale-independent and thus its action has no mass term (i.e. no term proportional to an operator squared) or, for that matter, any term whose coeffiecient has a dimension other than 0, since any dimensionful coefficient would specify a scale. To this action, however, we would like to add a deforming term corresponding to our ϕ field at the boundary; namely, we would like to add a term that looks like

$$S_{\text{deform}} = \int_{\mathbb{Q}_p} dy\, \phi'(y)\mathcal{O} \tag{6.96}$$

where $\mathcal{O}$ is some operator whose coefficient is given by ϕ', and ϕ' is the value of the ϕ field on the boundary of the tree, which we will assume has the form

$$\phi' \sim \phi(x_n, x_0)|x_0|_p^{\Delta_\phi - 1}. \tag{6.97}$$

In Eqn. 6.96, the ϕ' will act like a source for the $\mathcal{O}$ operator, and we can use functional derivatives of $e^{-S_{\text{deform}}}$ to compute correlation functions involving $\mathcal{O}$; this is done in Reference [9]. Here, we are merely concerned with what the value of Δ_ϕ means for this deformation.

Before we continue, however, we take a moment to justify our assumption of Eqn. 6.97. To do so, we consider the bulk-to-boundary propagator K_ϕ given in Eqn. 3.27. If we apply it to the field at a boundary point a and use it to propagate that field to a point (x_n, x_0) in

the bulk of the tree, we should find that this yields something proportional to the value of the ϕ field at x. To get the total value of the field at x, we should integrate over all possible boundary points a from which we could start our propagation. Therefore we write

$$\phi(x_n, x_0) = \phi' \int_{\mathbb{Q}_p} da K_\phi(x_n, x_0; a). \tag{6.98}$$

To actually perform this integration over the p-adics, we refer back to Section 2.3. In the cases in which $|x_0|_p \geq |a_n - x_n|_p$, our K_ϕ lacks any a dependence; this is true when a_n is any integer multiplied by x_0, namely when a can be reached by a direct ascent from x. In all other cases, we can represent our denominator as $(p^m|x_0|_p)^{2\Delta_\phi}$, where m is some positive integer; this is because p-adic norms are always a power of p, and since we are in a region where $|a_n - x_n|_p \geq |x_0|_p$, $|a_n - x_n|_p$ must be greater by a positive power of p, namely p^m. Also, for the sake of simplicity and without loss of generality, we take x_n to be 0, meaning that the point x will lie on the trunk of the tree. This means we can separate our integral as

$$\begin{aligned}\int_{\mathbb{Q}_p} da \frac{\zeta_p(2\Delta_\phi)}{p^{\Delta_\phi}} \frac{|x_0|_p^{\Delta_\phi}}{|\sup(x_0, a_n - x_n)|_p^{2\Delta_\phi}} = \\ \frac{\zeta_p(2\Delta_\phi)}{p^{\Delta_\phi}} |x_0|_p^{-\Delta_\phi} \int_{x_0\mathbb{Z}_p} da + \sum_{m=1}^{\infty} \frac{\zeta_p(2\Delta_\phi)}{p^{\Delta_\phi}} \frac{|x_0|_p^{\Delta_\phi}}{p^{2\Delta_\phi m}|x_0|_p^{2\Delta_\phi}} \int_{x_0 p^{-m}\mathbb{U}_p} da\end{aligned} \tag{6.99}$$

Since $\mathbb{Z}_p$ represents all points rooted at or above the point $(0, p^0)$, the quantity $x_0\mathbb{Z}_p$ represents all the points rooted at or above $(0, x_0)$, which means that the first integral represents the integral over all a that can be reached from x by going directly upwards. Furthermore, $\mathbb{U}_p$ represents all numbers rooted at p^0; therefore, $x_0 p^{-m}\mathbb{U}_p$ represents all numbers rooted at a point m steps below x_0. Between these two integrals, we have covered all possible boundary points a.

The first integral, using Eqns. 2.7 and 2.8, simply integrates to $|x_0|_p$. The integrals in the second term, from Eqns. 2.8 and 2.10, become $|x_0|_p p^m \left(1 - \frac{1}{p}\right)$. Thus our integral becomes

$$\begin{aligned}\int_{\mathbb{Q}_p} da \frac{\zeta_p(2\Delta_\phi)}{p^{\Delta_\phi}} \frac{|x_0|_p^{\Delta_\phi}}{|\sup(x_0, a_n - x_n)|_p^{2\Delta_\phi}} = \\ \frac{\zeta_p(2\Delta_\phi)}{p^{\Delta_\phi}} |x_0|_p^{-\Delta_\phi+1} + \frac{\zeta_p(2\Delta_\phi)}{p^{\Delta_\phi}} |x_0|^{-\Delta_\phi+1} \left(1 - \frac{1}{p}\right) \sum_{m=1}^{\infty} p^{-m(2\Delta_\phi - 1)}\end{aligned} \tag{6.100}$$

Combining terms and computing the infinite sum, we find

$$\int_{\mathbb{Q}_p} da \frac{\zeta_p(2\Delta_\phi)}{p^{\Delta_\phi}} \frac{|x_0|_p^{\Delta_\phi}}{|\sup(x_0, a_n - x_n)|_p^{2\Delta_\phi}} = \frac{\zeta_p(2\Delta_\phi)}{p^{\Delta_\phi}} |x_0|_p^{-\Delta_\phi+1} \left(1 + \left(\frac{p-1}{p}\right)\left(\frac{p^{-2\Delta_\phi+1}}{1-p^{-2\Delta_\phi+1}}\right)\right) \tag{6.101}$$

We are not concerned here with the various constants; see Equation 39 in Reference [9] for a more careful analysis of the constant terms. What is important to us is the scaling, namely that

$$\phi(x_n, x_0) \sim \phi' |x_0|_p^{-\Delta_\phi+1}, \tag{6.102}$$

which we see is exactly what we wanted from Eqn. 6.97.

We are now ready to proceed with our analysis of the effects of Δ_ϕ, and to do so, let us perform some dimensional analysis. Our ϕ field has dimension 0, which we can see by first noting that the first term in Eqn. 5.14 is proportional to $\frac{1}{b}$. Since the action as a whole should be unitless, this implies that b is unitless. This in turn implies, because of the second term in the action, that ϕ is unitless. Since we consider x_n to be a kind of length in the 1-dimensional boundary space, it must have dimension $(\text{mass})^{-1}$; therefore, Eqn. 6.97 implies that the dimension of ϕ' is $1 - \Delta_\phi$. Since we want our deformation action to be unitless, and since the integral contributes a dimension of $(\text{mass})^{-1}$, we conclude from Eqn. 6.96 that $\mathcal{O}$ must have dimension Δ_ϕ. We would like this operator to be relevant in the CFT, and so therefore we would like its coefficient, ϕ', to have mass dimension ≥ 0. This only happens when $\Delta_\phi < 1$. Furthermore, in the ordinary Archimedean (non-p-adic) case, we cannot have operators with negative mass scaling dimensions. Although we are not sure that this is true in the p-adic case, it seems likely to cause problems in the CFT, and therefore we assume here that Δ_ϕ must be greater than 0. Therefore we have the restriction that $0 < \Delta_\phi < 1$ for scalars that have a relevant dual operator the CFT. This restriction is exactly the one we obtained in previous sections from our boundary analysis! As a result, we find that having a negative mass squared term in our bulk action corresponds to the operator that is dual to that scalar field being relevant in the CFT we consider on the boundary.

Furthermore, if we add a relevant operator $\mathcal{O}$ to our conformal action, the action is no longer independent of scale, since we now have a dimensionful parameter that will change values as we change energy scales; this is what is known as a renormalization group flow. If we consider a CFT on the boundary of the Bruhat-Tits tree, we can correlate a length scale

in the CFT with a depth in the tree. That is to say, in order to travel from one boundary point to another via the tree, we must descend into the tree to a common ancestor and then ascend back to the boundary. If we only have to descend a few steps into the tree before being able to turn around and ascend up a different branch, then in a sense our start and end boundary points are "close." Conversely, if we must descend many steps into the tree before we can turn around, then our start and end points are "far." Note that we assume we take the minimal path from one point to another, so that we never retrace an edge. Therefore, we consider the value of $\tilde{\phi}$ at a given level to correspond to the coupling constant for $\mathcal{O}$ at the distance scale that corresponds to that depth in the tree.

One way we can envision renormalization group flow in this picture is in analogy to the Wilsonian renormalization approach. In Wilson's picture, we imagine computing all our quantities assuming that particles have an momentum less than some high momentum cutoff Λ. To find how our coupling constants change with scale, we imagine integrating over all momenta $c\Lambda < k < \Lambda$ where $0 < c < 1$. In doing so, we are effectively "integrating out" particles with momentum less than Λ but greater than $c\Lambda$ (typically c is close to 1). This process can be repeated many many times, and the way in which the effective coupling constant changes determines the renormalization group flow.

Analogously, we can have some depth level cutoff λ in our tree such that we require all particles in our CFT to descend to at least this level in the tree before ascending again to another boundary point. This sets a cutoff for how fine of a lattice a particle can see; a deeper (larger) λ corresponds to a coarser lattice on the boundary. Furthermore, since momentum is inversely proportional to distance, by imposing a minimum depth requirement (asserting we must travel to at least depth λ), we have effectively imposed a maximum momentum requirement. Therefore, we can perform a coupling constant rescaling by integrating over one or more levels of points, for example by integrating over the λ level so that our new minimum level we must descend to is $\lambda + 1$.

If we assume a depth-dependent solution for the ϕ field, as in Section 6.1, we see that at some depth our coupling (ϕ_i) becomes very large; however, as we mentioned in the section, our solution is necessarily incomplete, and cannot be trusted once we get outside the range where pertubation theory is applicable. However, for the radially symmetric and almost-tree solutions, we note that as we integrate over each layer of the tree, our coupling strength approaches the value of the central point (or the ring), which is finite. In fact, our renormalization group flow is cut off at the center, because we cannot go to "longer" distances or higher energies; once we have descended to the center, we cannot

descend further. On the CFT side of the correspondence, this is a result of the fact that our boundary has only a finite volume when we assume a radially symmetric solution; changing the kind of symmetry we expect in the bulk corresponds to changing the conformal frame in the CFT, and the conformal frame corresponding to radial bulk symmetry has a finite volume. This meshes with the fact that our renormalization group flow is cut off at low energy, or large distance, because at large enough length scales the CFT is affected by the finite size of its volume and cannot flow to longer distance scales.

Chapter 7

Conclusion

This thesis has explored some of the implications of p-adic AdS/CFT, and in particular has worked out a full classical theory of gravity on the 2-dimensional Bruhat-Tits tree, the equivalent of an AdS space with a boundary corresponding to the p-adic numbers. In this thesis, we have computed the bulk-to-bulk and bulk-to-boundary propagators for both the ϕ and J fields, which we have seen can aid in calculating the relationship of the fields to the corresponding CFT. Most importantly, this thesis has taken a natural extention of the work done in [1], in which the authors developed the Einstein field equation on the Bruhat-Tits tree in the absence of matter, and in this thesis we have proposed an equivalent of the Einstein field equation for the tree that includes matter (Eqn. 5.14). Furthermore, we have found some interesting solutions to this Einstein equation. Our solutions, obtained by perturbative methods, show us that we can have solutions for our fields that, at the boundary, appear to be very close to spacetime with constant negative curvature ($J_{xy} = 1$) that is devoid of matter ($\phi_x = 0$); these solutions become more perturbed further from the boundary.

We acknowledge that a depth-dependent exponential solution (found in Section 6.1) is necessarily limited, because the exponential will eventually become large at extreme values of i and our perturbative approach will break down. Therefore, more work is needed to find consistent solutions that are depth-dependent on the tree. One possibility, which is perhaps the most elegant and attractive, is a solution that approaches constant edge lengths infinitely far up and infinitely far down in the tree with exponentially small deviations (though the constant lengths may be different in each direction). In this solution, the scalar field in each direction will likely also fall off exponentially (though again, potentially settling around different values in opposite directions). In the middle, where neither of

these behaviors dominates over the other, we will likely find a non-perturbative solution that acts as a transition between these two exponential behaviors. Such a behavior would correspond to a transition from one conformal "fixed point" high up in the tree to another one very deep in the tree, hence the attractiveness of this possibility; however, we do not have strong reasons to believe such a solution must exist, as they will likely require precise tuning of our potential $V(\phi)$.

Our solutions for both the tree and the almost-tree in which we assume radially symmetric solutions (Sections 6.2 and 6.3), however, do not inherently encounter such complications, and therefore our solutions to these are valid solutions everywhere on the graph (approximately, as we relied on perturbation theory to arrive at these solutions). Further research should be done into investigating possible non-perturbative solutions in these geometries, as our work in this thesis shows that solutions with these geometries can exist self-consistently, and any non-perturbative solution should approximate our perturbative solution far out in the tree.

Much more can and should be done on this subject. These calculations were done with a 1-dimensional boundary and a 2-dimensional bulk; a fairly easy step would be to generalize these equations to higher dimensions, using the unramified extension of the p-adic numbers. Beyond this, the non-perturbative calculations mentioned in the previous paragraph would all provide valuable insight into the possible behavior of the fields inside the tree. Furthermore, there may be other geometries that would give reasonable and valid solutions. For example, Section 5 of Reference [1] finds an unusual edge length prescription that satisfies the Einstein equation with no matter, and we could consider taking this as our background solution instead of all $J_{xy} = 1$; doing so would lead to a different set of perturbative solutions. Other solutions that depend on different field configuration assumptions or on different geometries may also be possible. For example, Heydeman et al. propose tree geometries similar to the almost-tree presented here, but with a more complicated sub-graph in the middle. For instance, instead of a simple ring in the center of a diagram like that shown in Fig. 6.5, we might have 2 rings that share an edge in the middle, or more rings connected in such a way, and it would be worthwhile to see if similar solutions to those found on the almost-tree can be applied to these more complicated geometries [13].

A deeper exploration of what implications each of these solutions would have for the equivalent conformal field theory would also be a fruitful and worthwhile avenue of further research. This thesis has begun this investigation by showing that solutions for which

$r < 0$ correspond to adding a relevant operator to the CFT, which in turn will cause a renormalization group flow. In fact, in the radially symmetric and almost-tree situations, this flow has a definite cutoff as well. We can ask, and perhaps in future work search for, what the termination of the flow in the depth-dependent case might be. Depending on our potential $V(\phi)$, perhaps we will find some fixed point(s), or perhaps there is no termination of the flow.

Finally, our action on the tree (Eqn. 5.12) was hand-picked to produce equations of motion that are analagous to gravity on the tree, and this has informed us a great deal. However, even better would be a derivation of what properties any action on the tree must have, and how these properties would correspond to the related CFT on the p-adic boundary. This would give us an indication for how to generalize our Einstein equation and the results presented here to a generic tree action, and this might inform us as to what larger implications these results might have for the AdS/CFT duality.

Appendix A

Equivalence of Graviton Actions

Here, we aim to show that our Einstein-Hilbert action, given by Eqn. 5.7, is equivalent to our naive graviton action given by Eqn. 4.4, assuming for the former action that our graviton values J_{xy} are very close to 1, such that Eqn. 5.8 is true for $j_{xy} \ll 1$, and assuming in the latter action that the graviton is massless ($m_J = 0$). We have reproduced Eqns. 5.7 and 4.4 here for convenience:

$$S_G = \sum_{\langle xy \rangle} \left[\frac{\sqrt{J_{xy}}}{\sum_i J_{xx_i}} \left(2\sqrt{J_{xy}} - \sum_i \sqrt{J_{xx_i}} \right) + \frac{\sqrt{J_{xy}}}{\sum_i J_{yy_i}} \left(2\sqrt{J_{xy}} - \sum_i \sqrt{J_{yy_i}} \right) - 2\Lambda \right], \tag{A.1}$$

$$S_J = \frac{1}{2} \sum_{\langle\langle xy \rangle\langle yz \rangle\rangle} (J_{xy} - J_{yz})^2 + \frac{1}{2} \sum_{\langle xy \rangle} m_J^2 J_{xy}^2. \tag{A.2}$$

For further convenience, we introduce the notation

$$\kappa_{x \to y} \equiv \frac{\sqrt{J_{xy}}}{\sum_i J_{xx_i}} \left(2\sqrt{J_{xy}} - \sum_i \sqrt{J_{xx_i}} \right) \tag{A.3}$$

such that

$$\kappa_{xy} = \kappa_{x \to y} + \kappa_{y \to x}. \tag{A.4}$$

We first take the ansatz that $J_{xy} = 1 + j_{xy}$ for some small value of j_{xy}, and we use this to expand Eqn. A.1 in powers of j_{xy} through order j_{xy}^2. We will do so with only $\kappa_{x \to y}$ for now; $\kappa_{y \to x}$ is expanded analogously, and Λ is a constant that does not need expansion.

Thus, $\kappa_{x\to y}$ becomes:

$$\begin{aligned}\kappa_{x\to y} =& \frac{1}{p+1}\left[1-\frac{\sum_i j_{xx_i}}{p+1}+\frac{(\sum_i j_{xx_i})^2}{(p+1)^2}\right] \\ &\times\left[2\left(1+j_{xy}\right)-\left(1+\frac{1}{2}j_{xy}-\frac{1}{8}j_{xy}^2\right)\left(p+1+\sum_i\frac{1}{2}j_{xx_i}-\sum_i\frac{1}{8}j_{xx_i}^2\right)\right]\end{aligned} \tag{A.5}$$

Multiplying out and keeping only terms second-order or less in j, this simplifies to

$$\begin{aligned}\kappa_{x\to y} =& \frac{1}{1+p}\Bigg[1-p+ \\ &\left(\frac{3-p}{2}\right)j_{xy}+\frac{p-3}{2(p+1)}\sum_i j_{xx_i}+ \\ &\frac{p+1}{8}j_{xy}^2+\frac{1}{8}\sum_i j_{xx_i}^2+\frac{3-p}{2(p+1)^2}\left(\sum_i j_{xx_i}\right)^2+\frac{p-7}{4(p+1)}j_{xy}\sum_i j_{xx_i}\Bigg]\end{aligned} \tag{A.6}$$

The action in Eqn. A.1 is represented as a sum over all pairs of vertices, and we note that for any given edge g, the length of g appears in multiple terms of our sum. That is to say, when both x and y are endpoints of g, terms of the form j_{xy} contribute; however we also get contributions when either x or y is an endpoint of g in the form of j_{xx_i} or j_{yy_i}. Therefore, let us now count the overall contribution to S is that is made by any particular g. We would like to look at three kinds of terms: those proportional to g, those proportional to g^2, and those proportional to gh, where $h\sim g$. We ignore the constant as an irrelevant shift.

For our g terms, remember first that we must consider contribitions from both $\kappa_{x\to y}$ and $\kappa_{y\to x}$. Thus, we will have 2 terms like the first term in the second line of Eqn. A.6, one from each κ. We will also have $2(p+1)$ terms like the second term in line 2 of Eqn. A.6, because there will be $(p+1)$ edges that include x as one of its vertices, and each of these edges will have a term like the second term in the second line of Eqn. A.6. This holds for y as well, and thus we have $2(p+1)$ of these terms in total. Adding these together, we find the total coefficient of the term proportional to g in the action S is

$$\frac{1}{p+1}\left[(2)\left(\frac{3-p}{2}\right)+(2(p+1))\left(\frac{p-3}{2(p+1)}\right)\right]g=0. \tag{A.7}$$

Thus we conclude there are no terms that contribute to the action that are linear in j.

For our g^2 terms, we find that we will have 2 copies of the first term from line 3 of Eqn. A.6, one from each κ. We should find $2(p+1)$ copies of the contribution from the second term, since this term is the sum of the squares of all edges connected to x. Since there are

$(p+1)$ edges connected to x, the sum that includes g^2 will be present in $(p+1)$ $\kappa_{x\to y}$'s; the same logic holds true for the $\kappa_{y\to x}$'s as well. The same logic applies to the third term as well, and so we find we will get $2(p+1)$ of those terms as well. In the last term, since j_{xy} must be our g in order for this to produce a g^2 term, we only get 2 contributions from this term, one from each κ. In total, then, our g^2 term will look like

$$\begin{aligned}
&\frac{1}{p+1}\left[(2)\left(\frac{p+1}{8}\right)+(2(p+1))\left(\frac{1}{8}\right)\right.\\
&\qquad\left.+(2(1+p))\left(\frac{3-p}{2(p+1)^2}\right)+(2)\left(\frac{p-7}{4(p+1)}\right)\right]g^2\\
&=\frac{1}{4(p+1)^2}\left[p^2+2p+1+p^2+2p+1+12-4p+2p-14\right]g^2\\
&=\frac{1}{4(p+1)^2}\left[2p^2+2p\right]g^2\\
&=\frac{p}{2(p+1)^2}g^2
\end{aligned}\tag{A.8}$$

Finally, we look at terms of the form gh, where g and h are neighbors. Looking again at the third line of Eqn. A.6, the first two terms will never contribute becuase they only involve squares of edge lengths, never cross products. The third term, however, will contribute $2(p+1)$ times for any given g and h. This is because this summation will appear in $p+1$ terms in the action, as there are $p+1$ edges that include x as an endpoint, and each will have this exact sum; the factor of two is from the fact that when we square a sum, cross products pick up a factor of 2. Note that we are only concerning ourselves with $\kappa_{x\to y}$, because we have implicitly assumed that g and h share the vertex x, which we can always make true based on our choice of which vertex to label x. The final term will contribute twice, once when g is the edge that appears as j_{xy} and once when h appears as j_{xy}. Thus, in total our coefficent for the gh term is

$$\begin{aligned}
&\frac{1}{p+1}\left[(2(p+1))\left(\frac{3-p}{2(p+1)^2}\right)+(2)\left(\frac{p-7}{2(p+1)}\right)\right]gh\\
=&\frac{1}{2(p+1)^2}\left[6-2p+p-7\right]gh\\
=&\frac{-1}{2(p+1)}gh.
\end{aligned}\tag{A.9}$$

Having done all of this work, we can finally rewrite Eqn. A.1 in a somewhat more

intuitive form. As it currently stands, we have shown that we can write S_G as

$$S_G = \sum_{\langle xy \rangle} \frac{p}{2(p+1)^2} j_{xy}^2 + \sum_{\langle\langle xy \rangle\langle yz \rangle\rangle} \frac{-1}{2(p+1)} j_{xy} j_{yz}. \tag{A.10}$$

The specifications under the second summation tells us to sum over every pair of neighboring edges, counting each edge only once. If we lable edges explicitly instead of specifying them by their endpoint vertices, we can write this in a nicer form:

$$S_G = \frac{1}{2(p+1)} \sum_{\langle ef \rangle} \frac{1}{2} \left(j_e^2 - 2 j_e j_f + j_f^2 \right) = \frac{1}{2(p+1)} \sum_{\langle ef \rangle} \frac{1}{2} \left(j_e - j_f \right)^2 \tag{A.11}$$

In the first equality, we have put this equation in a form that is explicitly symmetric with respect to e and f so that it does not matter in what way we label the edges. Because each edge has $2p$ neighbors (p on each side), putting $j_e^2 + j_f^2$ into the sum over all pairs will give us $2p$ factors of g^2 for any given edge g; this is why the factor of p has disappeared and the factor of $\frac{1}{2}$ appeared.

We now see that this is equivalent to the kinetic term in Eqn. A.2, up to an overall multiplicative factor, which we can rescale the entire action by. Thus, we see that the action in Eqn. A.1 is equivalent to Eqn. A.2 with $m_J = 0$ (which makes sense as we expect gravitons to be massless), if we assume $J_{xy} = 1 + j_{xy}$.

Bibliography

[1] Steven S. Gubser, Matthew Heydeman, Christian Jepsen, Matilde Marcolli, Sarthak Parikh, Ingmar Saberi, Bogdan Stoica, and Brian Trundy. Edge length dynamics on graphs with applications to p-adic AdS/CFT. 2016.

[2] Sunil Mukhi. String theory: a perspective over the last 25 years. *Class. Quant. Grav.*, 28:153001, 2011.

[3] Juan Martin Maldacena. The Large N limit of superconformal field theories and supergravity. *Int. J. Theor. Phys.*, 38:1113–1133, 1999. [Adv. Theor. Math. Phys.2,231(1998)].

[4] S. S. Gubser, Igor R. Klebanov, and Alexander M. Polyakov. Gauge theory correlators from noncritical string theory. *Phys. Lett.*, B428:105–114, 1998.

[5] Edward Witten. Anti-de Sitter space and holography. *Adv. Theor. Math. Phys.*, 2:253–291, 1998.

[6] G. W. Gibbons. Anti-de-Sitter spacetime and its uses. In *Mathematical and quantum aspects of relativity and cosmology. Proceedings, 2nd Samos Meeting on cosmology, geometry and relativity, Pythagoreon, Samos, Greece, August 31-September 4, 1998*, pages 102–142, 2011.

[7] Matthias R. Gaberdiel. An Introduction to conformal field theory. *Rept. Prog. Phys.*, 63:607–667, 2000.

[8] Minos Axenides, E. G. Floratos, and S. Nicolis. Modular discretization of the AdS_2/CFT_1 holography. *JHEP*, 02:109, 2014.

[9] Steven S. Gubser, Johannes Knaute, Sarthak Parikh, Andreas Samberg, and Przemek Witaszczyk. p-adic AdS/CFT. *Commun. Math. Phys.*, 352(3):1019–1059, 2017.

[10] Yuri I. Manin and Matilde Marcolli. Holography principle and arithmetic of algebraic curves. *Adv. Theor. Math. Phys.*, 5:617–650, 2002.

[11] Daniel Harlow, Stephen H. Shenker, Douglas Stanford, and Leonard Susskind. Tree-like structure of eternal inflation: A solvable model. *Phys. Rev.*, D85:063516, 2012.

[12] L. Brekke and P. G. O. Freund. p-adic numbers in physics. *Phys. Rept.*, 233:1–66, 1993.

[13] Matthew Heydeman, Matilde Marcolli, Ingmar Saberi, and Bogdan Stoica. Tensor networks, p-adic fields, and algebraic curves: arithmetic and the $\mathrm{AdS}_3/\mathrm{CFT}_2$ correspondence. 2016.